Doctoral Thesis

Establishment of the Efficient Method to Produce Pseudopregnant Female Mouse

効率的な偽妊娠雌マウス作製法の確立

Gema Puspa Sari

Nara Institute of Science and Technology
Division of Biological Sciences
Organ Developmental Engineering
Associate Professor Ayako Isotani, PhD

Submitted on May 12th, 2022

Division of Biological Sciences Abstract of Doctoral Thesis

Laboratory (Supervisor)	Organ Developmental Engineering (Associate Professor Ayako Isotani, PhD.)		
Name	Gema Puspa Sari	Date	May 12th, 2022
Title	Establishment of the Efficient Method to Produce Pseudopregnant Female Mouse		

A Pseudopregnant mouse is a female mouse after copulated by sterile males, e.g., vasectomized (VAS) males. They are necessary for mouse strain production from the cryopreserved and in vitro fertilized embryos and for the generation of genetically modified mice that are useful and crucial in biomedical and behavioral research. Not only improving the health and welfare of humans and animals, but animal experimentations using mice are essential to understanding basic knowledge in biology that cannot be achieved with other techniques due to mice's anatomical, physiological, and genetic similarity to humans. Since the successful generation of gene-modified mice in early 1980 using assisted reproductive technology (ART), the number of mice utilized in experiments and gene-modified strains reported has been exponentially increasing. Therefore, advancing time- and cost-effective ART in mice is needed.

The embryo transfer technique in mice has been relatively unchanged for 50 years, and the preparation of pseudopregnant females as recipients remains an inefficient process. These females are essential for the embryo's development into the pup. However, to prepare pseudopregnant mice, females at the proestrus and estrus stages are selected before pairing with VAS males. Pseudopregnant mice can be recognized by the presence of a vaginal plug the following day after copulation. The precision of female mice selection depends on the operator's training, experience, and methods.

In this study, the relationship of the estrous cycle with successfulness in mating was examined. Mating will be considered a success when a vaginal plug is present the following day after pairing with VAS males. By estrous cycle staging by visual observation and vaginal cytology before pairing, we found that both mice on proestrus and estrus stages have a success rate of 64.1% and 63.7%, respectively. These results proved that vaginal cytology is a reliable method for evaluating the estrous cycle in the mouse.

Next, a new method to induce estrus synchronization was established using a Luteinizing Hormone-Releasing Hormone agonist (LHRHa). Estrous cycle synchronization is a process of targeting the female mammals to come to their receptive stages (stages when the female is receptive to her male counterpart for mating) simultaneously. LHRHa is similar to Gonadotropin-Releasing Hormone (GnRH), which will stimulate luteinizing hormone (LH) and follicular stimulating hormone (FSH) to be released from the anterior pituitary gland and induce ovulation and start the estrus stage. Since there is no report regarding the effect of LHRHa on the mouse estrous cycle, an optimal dose to induce estrus synchronization is needed to determine. Dosage of 0.02 mg LHRHa, administered through intraperitoneal injection, synchronized the estrus stage at 73.3% and the proestrus stage at 6.7%, four days after the treatment. While the dosage of 0.04 mg was showed 46.7% in the estrus stage and 13.3% in the proestrus stage. Thus, the dosage of 0.02 mg LHRHa was picked as the effective dose to synchronize the estrus stage in mice since the total percentage of the female mouse in the receptive stages (proestrus-estrus stages) was 80%.

Next, the effect of dose 0.02 mg LHRHa when administrated under three different conditions: 4-day (G1) before pairing, 3-day (G2) before pairing, and two consecutive day injections, 4- and 3-day (G3) before pairing was examined. G1 synchronized 80% of females in the estrus stage, while G3 synchronized 66.7% of females in the estrus stage and synchronized 13.3% of females in the proestrus stage (as for total, 80% of females were in receptive stages).

When these females were pairing with stud males, we found that 73% of G3 females showed vaginal plug on overnight pairing while G1 only 40%. Since receptive stages in female mice are on proestrus and estrus stages, G3 has an advantage in a higher probability of mating than G1. Furthermore, LHRHa treatment showed a little effect on embryo development since all pups from G1, G2, and G3 were born at standard pregnancy length, had an average litter size and body weight, and could survive during 24 h observation.

This study showed that estrus synchronization with 0.02 mg LHRHa by twice injection on two consecutive days (G3) has an excellent potential to be used as a protocol for estrus synchronization in the mouse. This study provides new information on methods to induce estrus synchronization for producing pseudopregnant mice. With increasing the efficiency of producing the pseudopregnant mice, the cost of maintaining a high number of mice can be reduced.

List of contents

List of figures

List of tables

Abbreviations

Conv	Convolutional
D	Diestrus
E	Estrus
FSH	Follicle stimulating hormone
GEMM	Genetically engineered mouse model
GnRH	Gonadotropin-releasing hormone
HPG	Hypothalamus-pitutary-gonadal
ICR	Institute of Canver Research – strain of mouse
ID	Identity
LH	Luteinizing hormone
LHRHa	Luteinizing hormone releasing hormone agonist
LHRHa 2x IP	LHRHa administration with intraperitoneal injection technique, dose 0.02 mg, and injected twice in two consecutive days and then paired 72 hours later with the male mice
LSD	Least significant difference
M	Metestrus
No.	Number
P	Proestrus
P<; P=	p-value, a statistical measurement used to validate a hyphothesis against the observed data
P4	Progesterone
PBS	Phosphat buffer saline
PMSG	Pregnant mare serum gonadotropin
VAS	Vasectomized

Chapter 1

Introduction

1.1. Pseudopregnant female mice

1.1.1. Definition of pseudopregnant mice

A pseudopregnant mouse is a female mouse that is bred with the vasectomized or infertile male mouse to result in sterile mating (Dewar, 1959). If the breeding is successful and the copulation happens, the vaginal plug (Figure 1.1.) can be observed the next day (Summa et al., 2012). The pseudopregnancy state can be achieved when the female mice are copulated by the infertile mouse, making its corpus luteum persists without an embryo (Dewar, 1973). As a result, the female mouse will behave hormonally pregnant, such as develop mammary glands, lactate, and build a nest, allowing its use as a recipient for the embryo transfer process in assisted reproductive technology (ART). In the absence of embryos, the corpora lutea will regress to increase the secretion of prostaglandin F2 alpha by the uterus (Critser et al., 1981), and progesterone will decline on the eight day (Greenwald and Rothchild, 1968). The pseudopregnancy state will end after 10-13 days, and the estrous cycle will continue (Dewar, 1959; Dewar, 1973). The pseudopregnancy state for mice is only common in laboratory mice because it is usually induced for the purpose of transplanting embryos into a surrogate mouse but is uncommon in wild mice because most of the wild males are fertile and will impregnate the female (Cunningham et al., 2007).

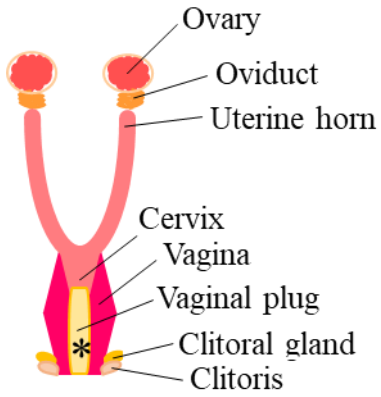

Figure 1.1. Simplified drawing of the female mouse genital system after copulation. Mouse vaginal plug (asterisk) fills the vagina with a slight protrusion into the mouth of the uterus (cervix). A vaginal plug can be observed in the next morning after breeding and if the copulation succeeds (Modified from Schneider et al., 2016).

1.1.2. Generation of the genetically engineered mouse model (GEMM)

A genetically modified mouse is a mouse (*Mus musculus*) that has had its genomes altered, such as knock-in, knock-out, and transgenic mouse, and is commonly known as genetically engineered mouse model (GEMM) (Sharpless and DePinho, 2006; Singh et al., 2012; Abate-Shen and Pandolfi, 2013). GEMM has an important part in biomedical research since it elaborates on basic biological processes and is used as models of human disease and studying the relationship between gene mutation and disease phenotype and drug developments (Figure 1.2., National Research Council, 1994).

The Number of GEMM has been increased since the 1980s with the advancement of assisted reproductive technology (ART) (Holt and Pickard, 1999; Yoshiki et al., 2009; Agca, 2012) and the development of the gene targeting knock-out technology (Thomas and Capecchi, 1987), and gene editing as general (Huijbers et al., 2015). Thus, genome editing technology increases the production of GEMM drastically as reported in Pubmed (Figure 1.3.).

GEMMs for biomedical research were bred in specific pathogen-free (SPF) animal facilities with certification that the colony is free from common pathogens that usually expose the wild animal on the same species (Lane-Petter, 1962; Dobson et al., 2019). This SPF method of breeding will exclude the disease or infection as an unwanted variable in the experiments (Scavizzi et al., 2021; Dobson et al., 2019). GEMM as a preclinical cancer model has helped the scientist to understand the immunotherapy effect as regiment cancer treatment and its dynamic with immune phenotype when the experiment was accomplished under SPF conditions (Murphy, 2016). To establish the SPF condition in generating GEMM, a “germ-free” condition is needed (Lane-Petter, 1962). One of the methods to get the “germ-free” condition when generating GEMM is by transferring the embryo into pseudopregnant mice to generate the GEMM pups.

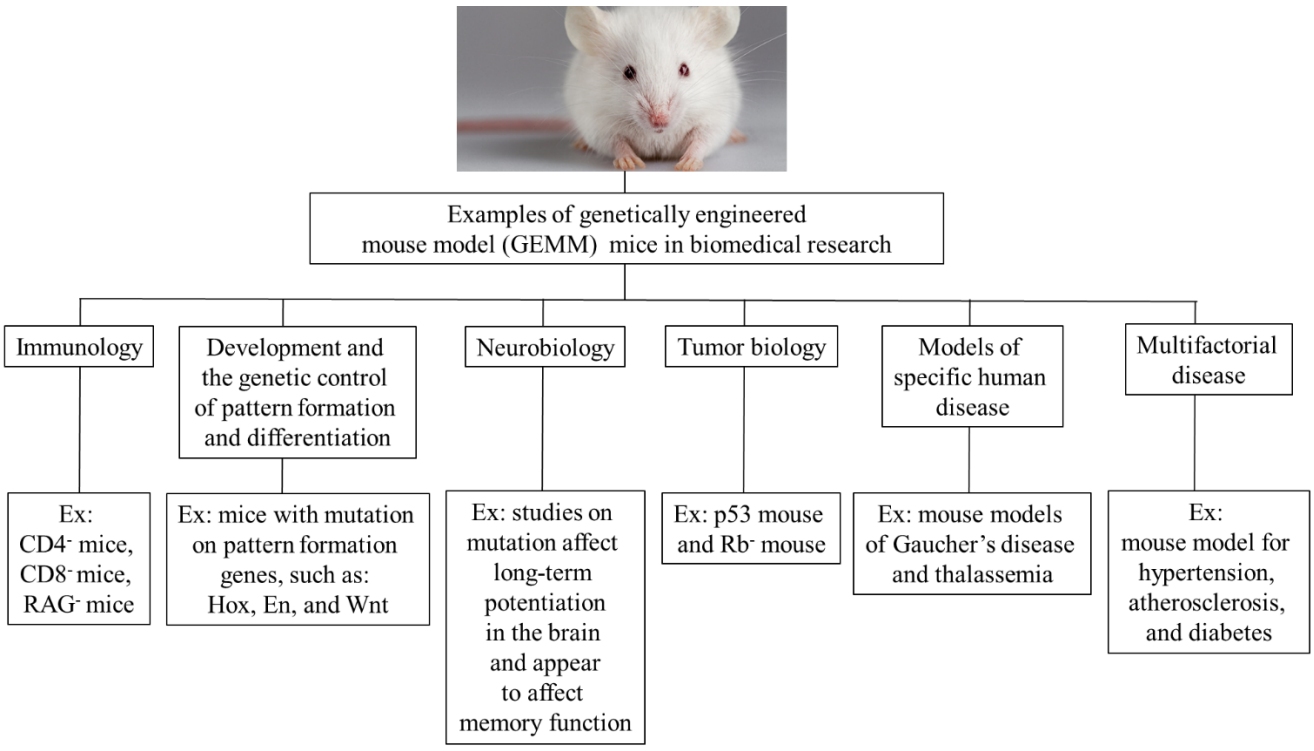

Figure 1.2. Impacts of GEMM in biomedical research. A few examples of how genetically engineered mouse models (GEMM) have had an impact on the conduct of biomedical research. (Modified from National Research Council, 1994).

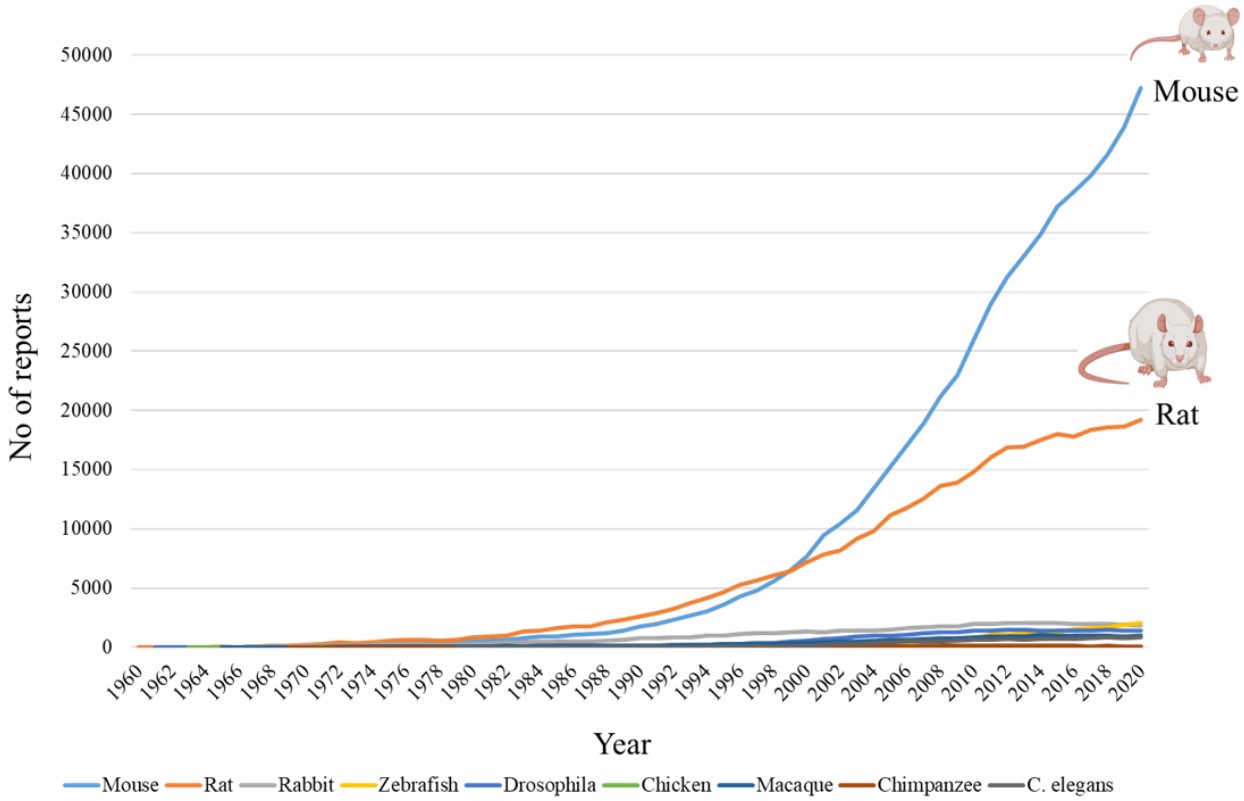

Source: Pubmed timeline results by year

Figure 1.3. Number of the report on the use of animals model from Pubmed. The Number of reports of the animal models from several animals: mouse, rat, rabbit, zebrafish, *Drosophila*, chicken, macaque, chimpanzee, and *C. elegans* from 1960-2020. Search query: 'animal model' + 'animal name'.

1.1.3. Production of pseudopregnant mice

ART and gene-editing technology such as CRISPR, Talen, and Prime editing not only increase the state of the art of knowledge of mice as an animal model but also increase the number of uses of the mouse itself for the study. While the ART is advancing with many technical improvements, such as increasing oocyte collection by improving superovulation protocol, production of GEMM still requires pseudopregnant female mice for the embryo transfer procedure, which has become an obstacle since its production is an inefficient process (Hasegawa et al., 2017). In pseudopregnant mice preparation, female mice in proestrus and estrus stages need to be selected to be paired with the VAS mice. While several methods, such as visual observation based on vagina appearance or vagina cytology, are used in the selection process, the precision of this selection process depends on the experimenter's training and experience (Hasegawa et al., 2017).

Another obstacle in producing the pseudopregnant mice is because the length of an estrous cycle in mice is normally 4-5 days, it is necessary to maintain about 4-5 times the number of females than the actual number that will be used in transfer embryo process (Hasegawa et al., 2017). Furthermore, when the pups are retrieved by Caesarean section at term, it is also necessary to prepare pregnant females as foster mothers on the same day or a few days before embryo transfer (Hasegawa et al., 2017). These make an effort and costs to produce the pseudopregnant mice high and not in line with the spirit of the principle of the 3R –reduction, refinement, and replacement (Flecknell, 2002).

1.2.Mouse estrous cycle

1.2.1. Staging of the estrous cycle

The estrous cycle in the mouse reproduction system is equal to the human reproductive cycle or menstrual cycle (ovarian and uterine cycles) and persists for 4-5 days in mice (Byers et al., 2012; Caligioni, 2009; Cora et al., 2015) (Table 1.1.). The term estrus was introduced by Heape (1900) when he reported that a mouse has four stages of estrus in an estrous cycle: proestrus, estrus, metestrus, and diestrus.

Table 1.1. Length of various stages of the estrous cycle in the mouse (Adapted from Cora et al., 2015)

Estrus Stages	Cycle length (hours)
Proestrus	< 24
Estrus	12-48
Metestrus	8-24
Diestrus	48-72

The reproductive period in female mice is marked with the start of the estrous cycle, which usually happens on their 26th day postnatal when the vagina starts to open. The increasing level of oestradiol is related to the vaginal unfolding process. Puberty is marked by the pulsatile release of luteinizing hormone (LH) around 30 days postnatal (Urbanski and Ojeda, 1985). Vaginal cell cornification, mediated by apoptosis, usually happens around ten days after vaginal opening and becomes a sign of puberty in the mouse or the first estrus or ovulation (Nelson et al., 1982). In the pregnancy stage, the phase will stay on diestrus. The short length of the estrous cycle makes the mouse become an ideal animal model to study the changes in the reproductive cycle (Caligioni, 2009).

From the study of 1000 cycles of unmated female albino mice, Parkes (1928) reported the length of the estrous cycle. About 45% of the population of all females have a 4-5 –day cycle with a combined proestrus-estrus stage average of 2.4 days and a combined metestrus-diestrus stage average of 3.7 days (Parkes, 1928). With the assumption that the average estrus stage is 14 hours, approximately 12-15% of randomly cycling females should be in the estrus stage at any time point on a 4-5 –day estrous cycle (Heykants and Mahabir, 2015).

Proestrus is the preparatory period for a mouse to enter the heat or estrus stage. Metestrus is a short period where corpus luteum function is declined when the pregnancy does not happen and then followed by diestrus, which is a period of brief rest during the estrous cycle. Some other animals have an anestrus stage, is a non-breeding period when reproductive organs are inactive (Heape, 1900). These estrus stages could be defined by behavioral (Meziane et al., 2007), morphological, and cytological changes in the mouse reproduction system (Byers et al., 2012; Ajayi and Akhigbe, 2020). Macroscopic changes or morphology can be seen in the vulva, such as vulva swelling and pinkish in the proestrus stage (Champlin et al., 1973; Byers et al., 2012). Microscopic or cytological changes as vaginal smears show different combinations of nucleated epithelial cells, cornified epithelial cells, and neutrophils (leukocytes) (Byers et al., 2012; Cora et al., 2015).

The follicular phase resembles the proestrus stage, which is associated with an increase in circulating estradiol level and little surge in prolactin. This leads to a rise in LH and Follicle Stimulating Hormone (FSH) release (Figure 1.4.). When FSH concentration is at its peak, estradiol levels rapidly decline and initiate the ovulation and estrus stage (Figure 1.4.). Metestrus and diestrus stages are associated with high levels of progesterone (Heape, 1900) (Figure 1.4.).

Nelson (1982) reported that sometimes 6-days cycles could be found on some mice, and mice have less regular cycle length than rats. On mice, a 4-day cycle is often followed by a 5-day rather than another 4-day cycle (Nelson et al., 1982). Estrous cycle length is influenced by age, nutrition, stress, social relationship, light, temperature, and noise (Cora, et al., 2015). For example, a mouse house as a single in each cage shows a cycle one day shorter than mice housed in the group (Nelson et al., 1982), and female mice have an estrous cycle more with the presence of male mice in the room (Whitten, 1956).

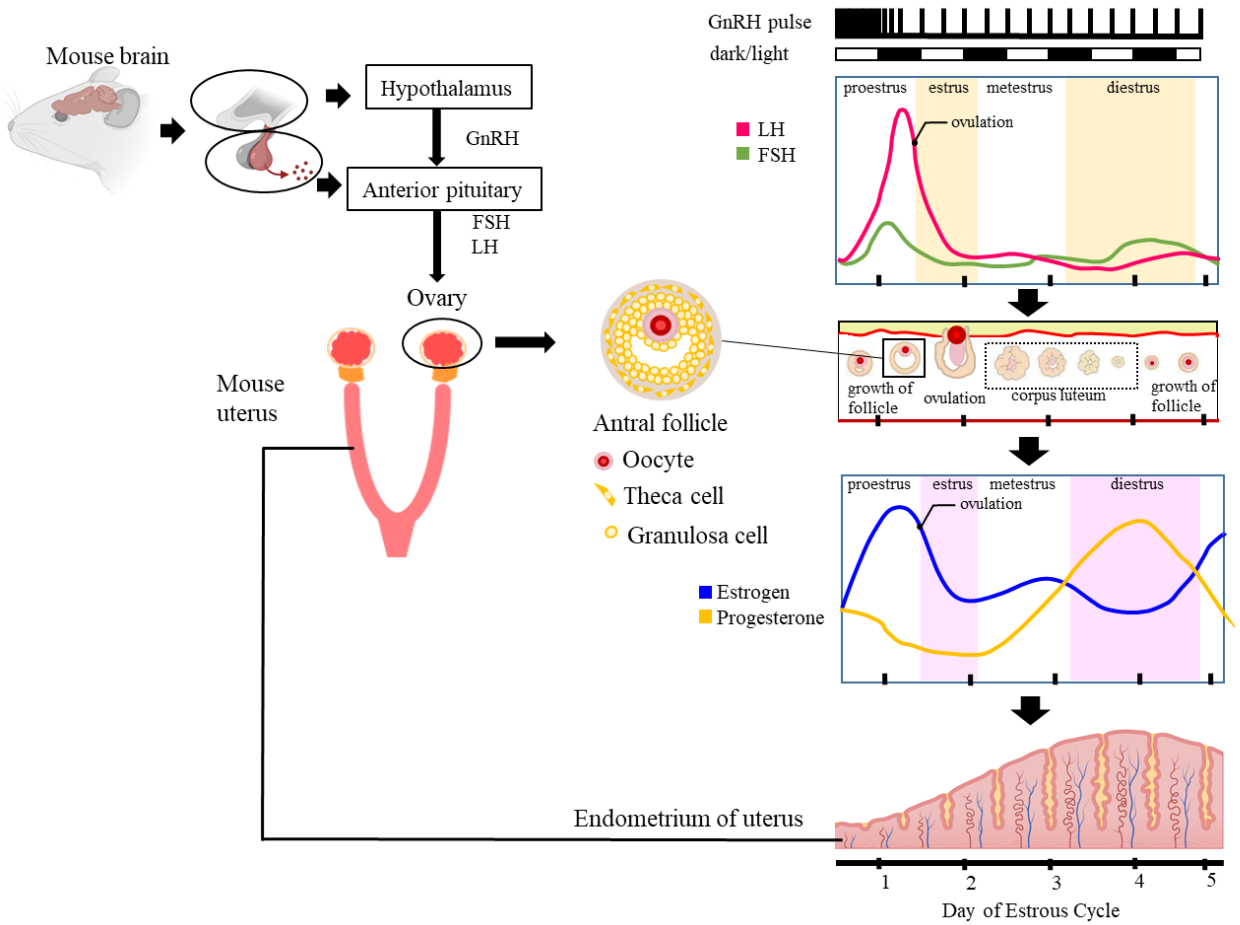

Figure 1.4. Estrous cycle in mouse related to hormonal, ovum, and endometrium changes. Hypothalamus will induce the production of GnRH, which will drive the secretion on LH and FSH by anterior pituitary. When LH and FSH levels increase, GnRH pulsatile will increase and lead to LH surge and drives the ovulation in the estrus stage. Progesterone and estrogen levels will increase during luteolysis when the corpus luteum is degraded (Modified from Urry et al., 2019; Miller and Takahashi, 2014).

1.2.2. Female hypothalamic-pituitary-gonadal (HPG) axis

The reproduction system is driven and directed by a neuroendocrine axis called the hypothalamus-pituitary-gonadal (HPG) axis. HPG axis consists of interaction between the hypothalamus and the anterior pituitary gland, which next drives the growth and maturation of germ cells, and production of steroids in female gonads.

Hypothalamus is a gland that secretes gonadotropin-releasing hormone (GnRH). It will trigger anterior pituitary glands to secret follicular stimulating hormone (FSH) and luteinizing hormone (LH). Next, FSH and LH will affect the granulosa and theca cells, respectively, to produce, which will induce estrus stage, progesterone, and estrogen (including estradiol and estrone). The positive feedback loop between estrogen and LH will prepare the follicle in the ovary and the uterus for the estrus stage, including ovulation and implantation (Figure 1.5.). The increasing level of progesterone and estrogen provides negative feedback to the hypothalamus and anterior pituitary glands and induces the diestrus stage (Figure 1.5.). This rapid rise in estrogen production by the ovaries and LH, called LH surge, drives the start of ovulation (Oyola and Handa, 2017).

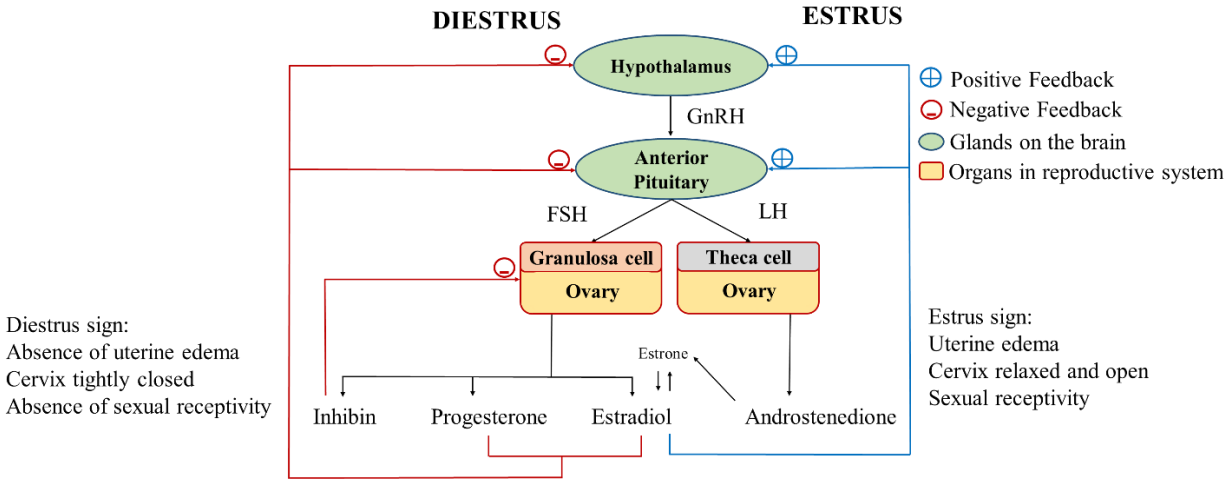

Figure 1.5. HPG axis and their interaction with the uterus in the non-pregnant mice. Hormones that are produced by the hypothalamus and pituitary will induce organs in the reproductive system to start the estrus stage by a positive feedback loop (blue arrow) and diestrus stage by negative feedback loop (red arrow) (Modified from Busato et al., 2017; Oyola and Handa, 2017).

1.2.3. Assessment of estrous cycle

The estrous cycle of the mouse consists of proestrus, estrus, metestrus, and diestrus and generally lasts for 4 to 5 days (Byers et al., 2012; Caligioni, 2009; Cora et al., 2015). With the assumption that the average estrus stage is 13 hours, approximately 12-15% of randomly cycling females should be in the estrus stage at any time point on a 4-5 –day estrous cycle (Heykants and Mahabir, 2015).

For small rodents, macroscopic findings and histological analysis are not suitable. Macroscopic by vaginal observation can be unreliable since it requires skillful and experienced investigators, and histological analysis is an invasive procedure and inappropriate for estrous cycle staging in live animals. Newer methods such as urine biochemistry and measurement of vaginal impedance are non-invasive methods. However, they show low reliability since not many studies reported the results of both methods. Urine biochemistry showed non-specific results and is unreliable because some rodent species show consistently high protein levels in their urine, which serve as chemical signals in these animals (Achiraman et al., 2018). Urine protein and lipid levels are significantly higher in the proestrus and estrus stages (Achiraman et al., 2018). The level of fatty acids in urine is higher in the estrus stage compared to other stages, while urine carbohydrate level is similar throughout the estrous cycle (Achiraman et., 2018). Measurement of electrical impedance on the vaginal wall is convenient, readily available, and requires less skill (Singletary et al., 2005). However, the apparatus is expensive and not widely accepted for the mouse because the probe was designed for rats (Jaramillo et al., 2012). Rats in the estrus stage have higher vaginal impedance than those in the non-estrus stages (Singletary et al., 2005; Jaramillo et al., 2012). In 1917, Stockard and Papanicolaou characterized the vagina changes during the estrous cycle through histology and cytology. The cytology method can solve the invasiveness problem and be suitable for live animals.

Identifying the estrous cycle stages is essential in selecting a female animal that will breed with the male to attain timed pregnancy and pseudopregnancy and identifying the estrous cycle as a variable that might affect the research (Byers et al., 2012). Several non-invasive methods have been reported to assess the estrous cycle in mice with high reliability. Two methods that are considered reliable methods are the visual method and the vaginal cytology method (Byers et al., 2012).

1.3. Determine the estrous cycle on mice and strategy to increase efficiency in pseudopregnant mice production

Several methods have been developed to accurately determine the estrous cycle stages. Champlin (Champlin et al., 1973) has reported the details of vagina appearance at each estrus stage. Thus visual assessment can be carried out while high skill and experience still needed. Assessment through vaginal cell type (Stockard and Papanicolaou, 1917) is still the most reliable method to determine the estrous cycle. In contrast, this method is time-consuming, and subjectivity among examiners is possible to happen. Some advanced techniques, such as the utilization of artificial intelligence, have also been developed to accurately determine the estrous cycle. If a high number of mice in the receptive stage is needed, the estrus synchronization technique can be used for the study.

1.3.1. Visual assessment

The visual assessment to observe vagina appearance in evaluating the estrous cycle is widely accepted and has been described by Champlin (1973) and summarized in Table 1.2. Visual assessment is considered the fastest method and can eliminate the risk of inducing pseudopregnancy or damaging the vaginal epithelium, especially with the swab method for collecting the vaginal cells.

A highly experienced and skillful observer in the Jackson Laboratory's Reproductive Science group can differentiate the mice in every stage of the estrous cycle and evaluated around 100 females in 10-15 minutes with no extra equipment or leaving the animal facility, with the result that more than 90% of mice determined in proestrus or estrus stage successfully mate overnight (Byers et al., 2015). However, for untrained experimenters, proestrus and estrus stages in some strains could be mistaken for late metestrus and diestrus stages (Champlin et al., 1973).

Tabel 1.2. The appearance of the vagina at different stages of the estrous cycle of albino mouse (Adapted from Champlin et al., 1973).

Estrous cycle	Vagina appearance
Proestrus	• Vagina tissues are reddish-pink and moist. • Vagina has gap (big opening) • There are numerous longitudinal folds or striation appear on the dorsal (oedematous/ swelling) and ventral lips
Estrus	• Vagina tissues are lighter pink and less moist • Vagina has gap, but the opening is smaller than in proestrus • The striation are more prominent
Metestrus	• Vagina tissues are pale and dry • The dorsal lip is not as oedematous as in the estrus • The dorsal lip is less oedematous and has receded • Whitish cellular debris may line the inner walls or partially fill the vagina
Diestrus	• Vagina tissues are bluish-purple in colour • Vagina is moist and has a small opening

1.3.2. Vaginal Cytology assessment

Determining the estrous cycle using vaginal cytology is accurate, reliable and has become a standard technique for identifying the estrous cycle in experiments. This method is laborious, time-consuming, and requires skillful examiners for microscopic examination of vaginal cells. Another disadvantage of this method is that subjectivity among the examiners could be challenging (Cora et al., 2015). The vaginal cells can be obtained by vaginal lavage (flushed), scrapping, or swabbing the mouse vagina. On the flushed method, the vaginal cells are flushed by gently pipetting a small amount of phosphate-buffered saline (PBS) into the vagina orifice, pipetted 4-5 times, and then smeared the fluid on the glass slide. In the swabbed method, the vaginal cells are obtained by carefully introducing PBS wetted cotton swab or scrapper to the vagina and then smeared into the glass slide. The glass slides are air-dried and stained with crystal violet stains, Toluidine blue O, or Wright's Giemsa. The glass slides were then washed to rinse extra staining. The observation was done under a light microscope (Cora et al., 2015).

There are three types of vaginal cells: neutrophils (leukocytes), cornified/ anucleated epithelial cells, and nucleated epithelial cells (in small or large size), as shown in figure 1.6.A-C. Nucleated epithelial cells can be found in small and round shapes or large and rugged shapes (Figure 1.6.A.). Cornified epithelial cells can be found as large and spread shapes or compacted bar shapes in early keratinization (Figure 1.6.B). Neutrophils are round, very small, and have multilobulated nuclei (Figure 1.6.C). During cell collection, neutrophils may condense or sometimes rupture. It is very important to recognize neutrophils' shape in every possibility to avoid misinterpretation of a particular stage. When the neutrophils are dominant and consistently observed, the stage is metestrus or diestrus, shown in figure 1.6.F-G, if neutrophils are rare to absent, the stage is either proestrus or estrus, as shown in figure 1.6.D-E (Adapted from McLean et al., 2012; Cora et al., 2015).

Small nucleated epithelial cells with round shapes are predominant on proestrus (Figure 1.6.D.). Infrequent neutrophils can be found in early proestrus, while on late proestrus, a relatively high number of large epithelial cells and cornified/ anucleated cells can be observed (Table 1.3. and Figure 1.6.). Estrus is characterized by predominant cornified epithelial cells (Figure 1.6.E.). Sometimes bacteria may be observed attached to the cells or free in the background. At the beginning of the estrus stage, the cornified cells are smaller (because they are folded into themselves, creating jagged elongated structures referred to as "keratin bars") and are typically

arranged in loose clusters. As the estrus progress, the cell number increase, and the size become larger and more evenly dispersed. In the late estrus, neutrophils may be observed (Figure 1.7.).

Metestrus is characterized by a combination of cornified epithelial cells and neutrophils. As metestrus progresses, neutrophils become very high and packed (figure 1.6.F.). However, in the late metestrus, the number of neutrophils and epithelial cells decreases and decreases in smear cellularity (figure 1.6.F.). Late metestrus and early diestrus are hard to distinguish (Cora et al., 2015). Diestrus is characterized by neutrophils, small and large nucleated epithelial cells, and a low number of cornified cells (figure 1.6.G.). In early diestrus, neutrophils may still appear clumped, and on late diestrus, neutrophils are sparsed and scattered with a low number of epithelial cells. During diestrus, viscous and stringy mucous are sometimes found, and the cells may be distorted along the string of mucous. Classification of the estrous cycle stages based on the cell types and relative cell density are summarized in Table 1.3., and a visual representation of cell types and relative proportion of each cell type present during the four stages of the estrous cycles is shown in Figure 1.7.

Table 1.3. Basic classification of the stages of the estrous cycle based on cell types and the relative number of these cells in vaginal smears of the mouse (Adapted from Cora et al., 2015).

Estrous Cycle	Neutrophils	Small nucleated epithelial cells	Large nucleated epithelial cells	Cornified epithelial cells	Relative density
Proestrus	0 to 1	2 to 3	0 to 1	0 to 1	Low to moderate
Estrus	0 to 1	0 to 1	0 to 1	2 to 3	Moderate to high
Metestrus	1 to 3	0 to 1	0 to 1	2 to 3	Moderate to high
Diestrus	2 to 3	1 to 2	1 to 2	0 to 1	Low to moderate

0 = none, 1 = few, 2 = moderate, 3 = high

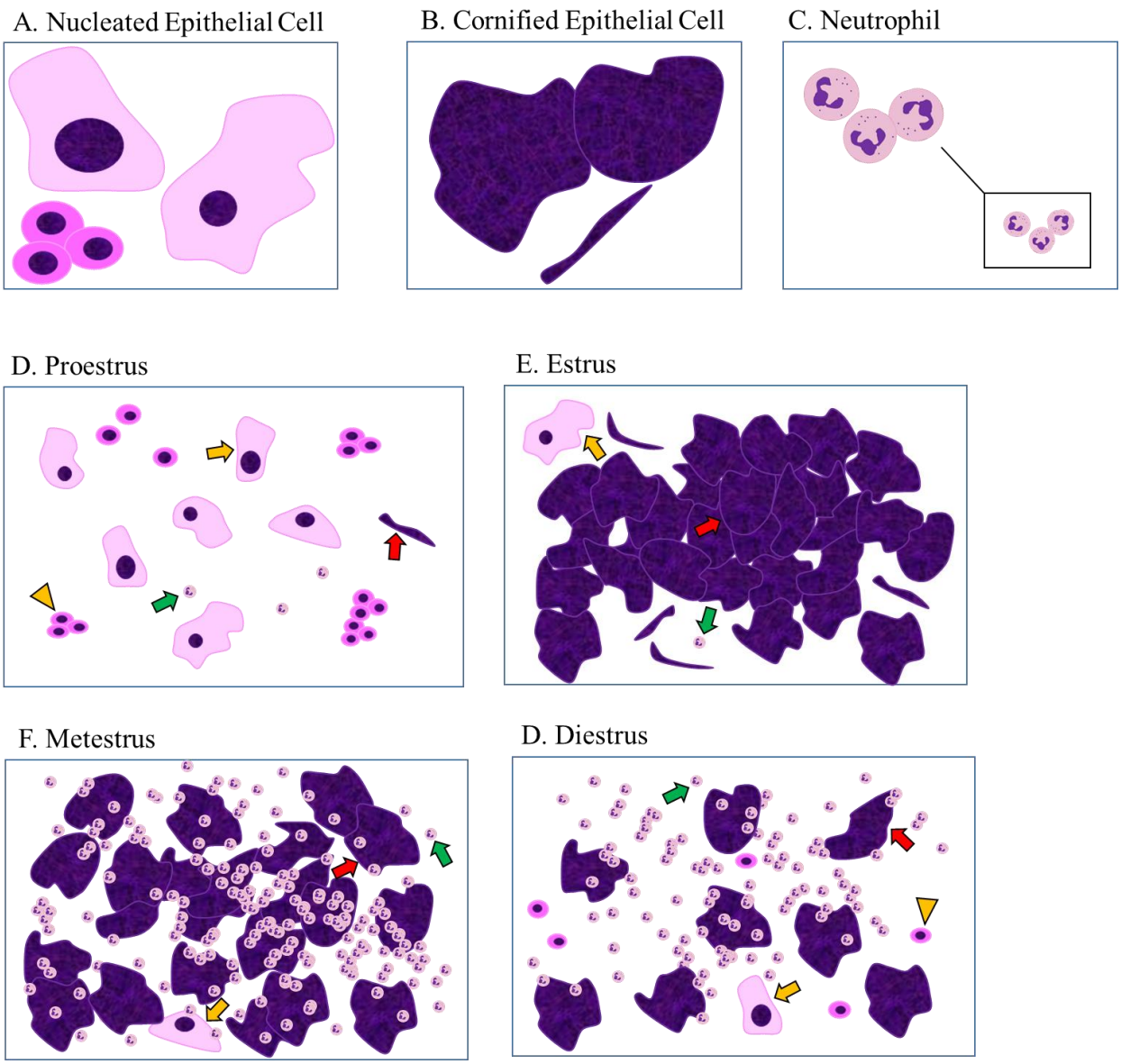

Figure 1.6. Cytological assessment of vaginal cells in identifying estrous cycle. Schematic picture of three main cell types in vaginal smear samples: (A) nucleated epithelial cell, (B) cornified epithelial cell, (C) neutrophils. The proportion of these cell types can be used to identify mice in (D) proestrus, (E) estrus, (F) metestrus, and (G) diestrus. The green arrow is neutrophils, the yellow arrow is large nucleated epithelial cell, the yellow arrow head is small nucleated epithelial cell, the red arrow is cornified epithelial cell (Modified from McLean et al., 2012; Cora et al., 2015).

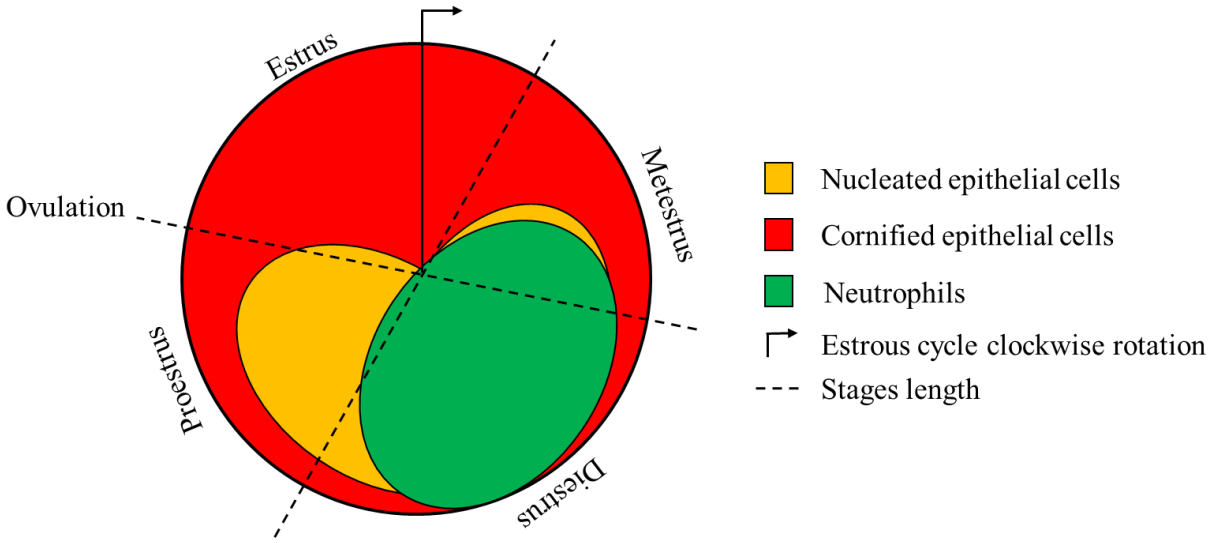

Figure 1.7. Estrous cycle stage identification tool. This diagram is visual representation of cell types and relative proportion of three cell types that present during four stages of estrous cycle. The dash line marks the stage changes of the estrous cycle. The arrow moves clockwise until the cell types and proportion appear under the arrow. Example, an arrow in the position 12 o'clock represents a vaginal smear all cornified epithelial cells and the mouse is in estrus stage. An arrow at 3 o'clock represents a smear combination of cornified epithelial cells, nucleated epithelial cells, and dominated by neutrophils and mouse is in metestrus stage (Modified from Byers et al, 2012; Sidibé et al., 2014).

1.3.3. Artificial intelligence for estrus detection

Computational advances and large-scale datasets have made dramatic progress in machine learning algorithms, especially in visual tasks such as object recognition and classification (Sano et al., 2020). Those algorithms have also been applied to medical fields. Their performance is comparably to or better than humans in some fields, including the diagnosis of skin rashes (Esteva, et al., 2017) the evaluations of chest X-rays (Rajpurkar, et al., 2017), and histopathological images (Ehteshami, et al., 2017; Liu, et al., 2019).

While the visual observation of vagina appearance and vagina cytology observation has become a common protocol in animal study, evaluating both methods by human examiners could be challenging because it needs a long training period to make a skillful examiner. The evaluation sometimes does not fully match among human examiners because of their subjectivity among them (Sano, et al., 2020). It makes computer-aided estrous stage classification could be a potential solution to the problem. Sano et al (2020) reported classifier of estrous stage using machine learning called "Stage Estimator of estrous Cycle of RodEnt using an Image-recognition Technique (SECREIT)", has succeeded to applied deep learning algorithms (Simonyan and Zisserman, 2019) to the automatic classification of the estrous stages. This system can distinguish diestrus, proestrus, and estrus stages in mice. SECREIT's performance was able to compare to skilled human examiners. SECREIT provided correct classification similar to that provided by two human examiners (SECREIT: 91%, Human 1: 91%, Human 2: 79%) in 11 s for a test using 100 images. However, this method still needed the vaginal cytology method. Thus, laborious and time-consuming still become the major issues.

1.3.4. Estrus synchronization

Estrus synchronization is the process of targeting female mammals to come to heat within a short time frame (36-96 hours). In generating GEMM, estrus synchronization will permit the efficient use of artificial insemination and embryo transfer procedures. The first estrus synchronization protocol is reported as the Whitten effect by Whitten (1956). On the Whitten effect, the pseudopregnancy occurs spontaneously when groups of female mice are housed together. Pseudopregnancy caused by the Whitten effect, also known as pseudopregnancy in a social setting, needs to be induced by tactile and pheromonal cues (Archunan and Dominic, 1991). In addition, continued exposure to pheromone is required to maintain them (Terkel, 1986) and must first be induced by the Lee-Boot effect (Lee and Boot, 1955; 1958), in which female mice are housed in group and isolated from males until they exhibit anestrus or a pressed or prolonged estrous cycle.

Estrous synchronization also can be achieved by exogenous hormone injection. Pallares and Gonzales-Bulnes (2009) reported two intraperitoneal doses of 0.5 µg of cloprostenol, three days apart, plus a single subcutaneous dose of 3 µg of progesterone coincidentally with the first injection of cloprostenol can induce ovulation. Wei et al. (2015) reported that injection of pregnant mare serum gonadotropin (PMSG) and cloprostenol intraperitoneally could induce estrus synchronization and uterine development. Hasegawa et al. (2017) reported that two subcutaneous 2 mg progesterone could induce ovulation and be used as recipients or surrogate mothers in embryo transfer.

Luteinizing hormone-releasing hormone agonist (LHRHa) has been known as an agent to regulate fertility since 1971 (Corbin and Bex, 1980) because of its ability to induce the release of pituitary LH and FSH that drives ovulation in a variety of animal models. Administration of 40 µg LHRHa subcutaneous at seven weeks of age Sprague-Dawley female rats showed synchronization in proestrus or estrus stages 96 hours later and confirmed copulatory plug after mating (Borjeson et al., 2014). However, no report has been found about the administration of LHRHa on the mouse for estrus synchronization.

1.4. Thesis rationale

The embryo transfer technique as one of the ART-related techniques in mice is still the same and needs pseudopregnant female mice as recipients to obtain mouse pups. Preparing the pseudopregnant female mice as recipients is an inefficient process. The reason is that the selection of females during the proestrus and estrus stages is made by visual observation of the morphology of the vagina before mating with the vasectomized male mice. Previously, Sano et al., (2020) developed an automatic classifier technique to determine the estrus stages in mice. However, their method still needs collecting and staining vaginal cells, which are tedious and time-consuming. While Sano et al., (2020) have high accuracy, an easier and faster method with high accuracy is still needed to determine the estrus stage in mice. This system might be unsuitable for preparing pseudopregnant mice in large numbers.

Thus, this study proposes a new method to increase the efficiency of pseudopregnant mice. I explored the vaginal cytology method to examine the correlation between the mating frequency and mouse estrous cycle based on the presence of a vaginal plug. Next, I explored LHRHa as a new agent to induce an estrous cycle synchronization in mice. This newly proposed method will increase efficiency in producing pseudopregnant mice by increasing the number of mice in receptive stages, which are proestrus and estrus stages. Thus, this study would contribute new information on new endocrinological agents or hormone treatment that regulate the mouse estrous cycle.

As part of this study, I also explored the possibility of applying machine learning to detect estrous stages in mice efficiently. Further, this can be a more comprehensive report in understanding the role of advanced technology in the biology reproduction field. The vulva or vaginal outer of female mice is different and changing according to the development of estrus stages. Estrus stage determination using an automation system will assess the estrous cycle of mice faster. Hopefully, this method will help the experimenter select mice in receptive stages even without special training. Thus, selecting mice in receptive stages can be done in any lab without depending on the human experimenter's skill or experience.

In summary, the main goal of this study is to accelerate the advancement in assisted reproductive technology, including in the development of GEMM, by providing an efficient new method to prepare the pseudopregnant mice.

Chapter 2 - Materials and Methods

2.1. Mice and animal guidelines

All animal experiments were conducted under the guidelines of "Regulations and By-Laws of Animal Experimentation at the Nara Institute for Science and Technology" and were approved by the Animal Experimental Committee at the Nara Institute of Science and Technology (the approval no.1639). Albino ICR mice are used in the present experiment. The mouse is maintained under 12 hours light/ 12 hours dark cycle (light on 08:00 am). The maximum caging density for female mice is five mice from the same litter and sex starting from weaning. Female ages are 8-24 weeks. Male vasectomized mice are prepared but cut their vas deferens. Food and water are available ad libitum.

2.2. Visual examination of the estrus stage

Visual examination of the estrus stage is performed based on criteria described by Champlin (Champlin et al., 1973, table 1.3.). Females mice are restrained on the cage grid with their front paws. By holding their tails, the rear end of the females was lifted slightly above the grid toward the observer. The vagina is observed under normal lighting, and the appearance of the vagina was photographed with a camera (CANON Powershot G9X). Visual examination and the digital image were examined at 08:00 am – 11:00 am and 02:00–04:00 pm.

2.3. Cytological examination of the estrus stage

Cytological examination of the estrus stage performed as described by Byers et al. (2012) with modification on cell transfer process to the glass slide. Vaginal cells are collected by swab method using a small size cotton-tipped wetted with room temperature phosphate buffer saline (PBS, Sigma) and inserted into the vagina of the restrained mouse. The cotton tip then turned and rolled carefully against the wall of the vagina. The cotton tip was then dipped into 25 ul PBS (Sigma). The vaginal cells were then transferred into a glass slide (Matsunami micro slide glass S2112), and then dried inside a 56°C oven for 20 minutes, and then stained with crystal violet (Merck 109218) for 90 seconds. The slides were washed carefully with tap water to rinse the excess staining. After drying, microscopic observation was done under a light microscope with 20 x magnification to observe all cell types (figure 1.2). The cell types in different stages of the estrous cycle are determined with the focus on the cell types that were characteristic of the different estrous stages, as described in table 3. Samples were collected from 08:00 am - 11:00 am.

2.4. Inducing pseudopregnancy

Pseudopregnancy was induced by pairing 8- to 16- week-old ICR females with vasectomized ICR (vas) males. ICR males are housed one per cage with a female introduced at 15:00 – 16:00 pm, and the vaginal plug was checked at 09:00 pm – 11:00 pm the following morning. Females are independently examined for the presence of a vaginal plug. The morning of plug detection is designated as 0.5 days of pseudopregnancy. Non-plugged mice are returned to stock for re-pairing in the following experiment. The schematic workflow is shown in Figure 2.1.

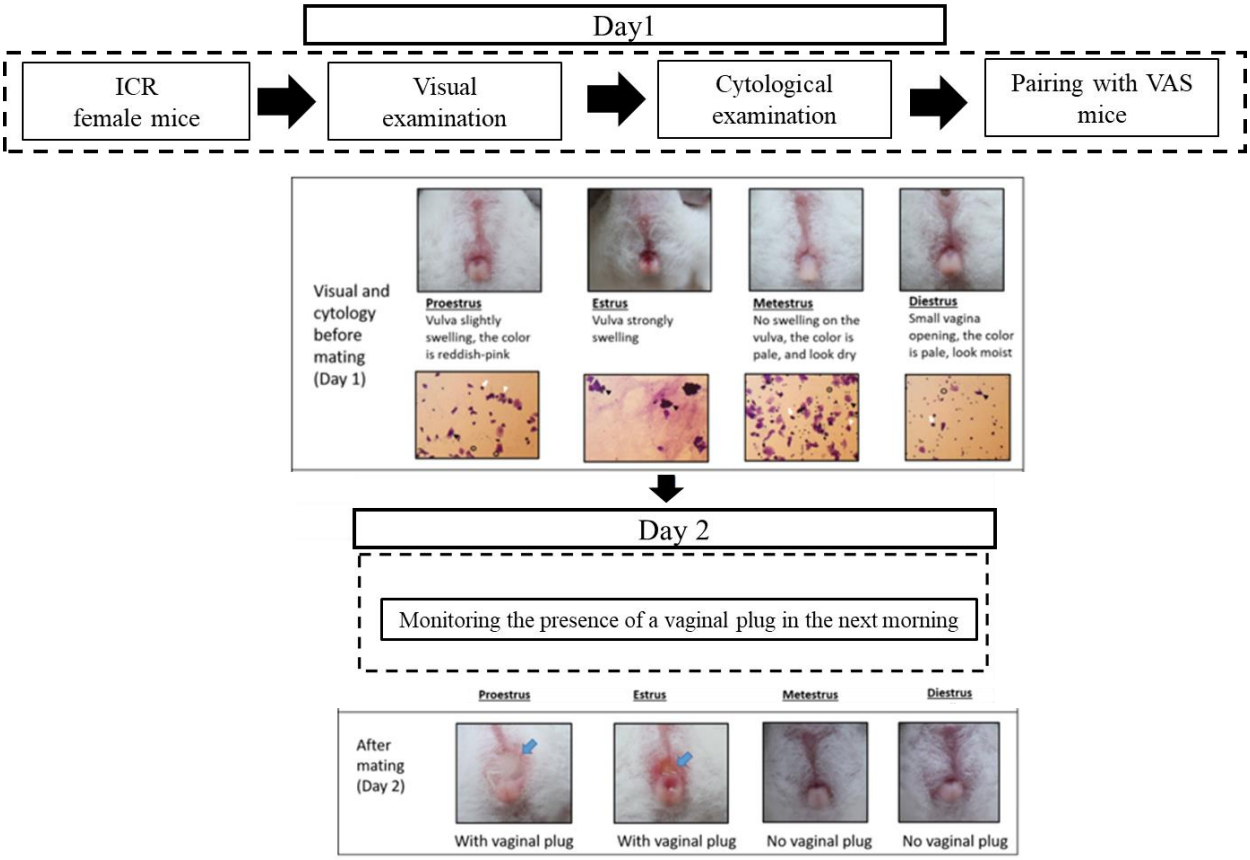

Figure 2.1. Schematic workflow for inducing pseudopregnancy experiment.

2.5. Optimization of LHRHa dose

ICR females mice aged 8-16 weeks were used. Four dose of LHRHa LHRHa (Glp-His-Trp-Ser-Tyr-Ala-Leu-Arg-Pro-NHEt; Sigma-Aldrich, L4513) were prepared: 0.005 mg, 0.01 mg, 0.02 mg, and 0.04 mg LHRHa. The injection was administrated in the afternoon between 11:00 am - 12:00 am, intraperitoneally on day 1. On day 5, the mice's estrous cycle stages were assessed by the vaginal cytology method, and then the mice were paired with stud ICR male mice.

2.6. Comparison of LHRHa treatment to other hormone treatment

ICR female mice aged 8-16 weeks were used. Five different treatments of hormone injection are described in table 2.3. Progesterone (P4; Proge depot 10 mg, Mochida Pharmaceutical Co. Ltd.) intraperitoneal injection was administrated to 2 mg for each mouse from 06:00 pm – 07:00 pm. The injection was done twice on day 1 and day 2 (Hasegawa et al., 2017). 5 IU PMSG (Aska Animal Health Co. Ltd.) intraperitoneal injection was administered to each mouse in 02:00 pm -03:00 pm (modified from Hasegawa et al., 2017). LHRHa (Glp-His-Trp-Ser-Tyr-Ala-Leu-Arg-Pro-NHEt; Sigma-Aldrich, L4513) intraperitoneal injection was administered in the afternoon between 11:00 am - 12:00 am for 01:00 pm - 02:00 pm to each mouse. Three different timing of injection, LHRHa_G1 (G1), LHRHa_G2 (G2), and LHRHa_G3 (G3), was performed to observe the effect of different timing or schedule of LHRHa administration (Table 2.1.).

On day 6, the mice's estrous cycle stages were assessed by the vaginal cytology method. On the same day, at 03:00 pm, the female mice were continuously paired with stud ICR male mice overnight (day 7). The presence of a vaginal plug was observed the following day after pairing (08:00 am - 12:00 pm). The female mice were taken back to their group and observed for their health and pregnancy. Two days before the delivered day, the mice were caged singly. Next, the litter size and weight of the offspring were examined. Two mice were prepared as control, without injection, but mating with stud ICR male as a comparison of the litter size and weight of the offspring. The schedule is summarized in Table 2.1.

Table 2.1. Injection schedule for hormone treatment dose

Treatment	Injection schedule (Day)					Pairing	Plug check
	1	2	3	4	5	6	7
Control (n=16)	Standard (Control)					Pairing	D7
5 IU PMSG (n=5)				PMSG		Pairing	D7
2mg progesterone (n=5)	P4	P4				Pairing	D7
0.02mg LHRHa_G1 (n=10)		LHRHa				Pairing	D7
0.02mg LHRHa_G2 (n=10)			LHRHa			Pairing	D7
0.02mg LHRHa_G3 (n=15)		LHRHa	LHRHa			Pairing	D7

2.7. Machine learning approach to classify estrous cycle to produce pseudopregnant mice

Dataset was prepared in ratio data training:test: 60:40, 70:30, and 80:20 with combining proestrus and estrus data (PE) and combining metestrus and diestrus data (MD). All data were prepared on separate folders named: TRAINING and TEST and subfolders: PE and MD.

Tabel 2.2. The total number of the digital images used

	Samples (Images)
Proestrus (P)	119
Estrus (E)	190
Metestrus (M)	59
Diestrus (D)	299

Table 2.3. Total number of the digital images used in the training, test, and validation

	Training			Test		
	Ratio 60	Ratio 70	Ratio 80	Ratio 40	Ratio 30	Ratio 20
PE	185	216	247	123	92	61
MD	214	250	286	143	286	190

Data preprocessing was done in the online cloud platform Google Colab (colab.research.google.com) for training the deep learning model that GPU can power. The datasets were uploaded to google drive. The model was built with Keras's implementation of VGG16 image classification architecture. Libraries were imported: cv2, NumPy, os. With the low number of images as data, the data was augmented during the training by ImageDataGenerator (by Keras) with parameters: zoom range = 0.15, width shift range = 0.2, height shift range = 0.2, shear range = 0.15). In VGG16, there are thirteen convolutional layers, five Max Pooling layers, and three dense layers, which sum up to 21 layers but have only sixteen weight layers (learnable parameters layer). It has convolution layers of 3×3 filter with a stride 1 and always uses the same padding and max pool layer of 2×2 filter of stride 2. It follows this arrangement of convolution and max pool layers consistently throughout the whole architecture. Conv-1 Layer has 64 number of filters, Conv-2 has 128 filters, Conv-3 has 256 filters, Conv 4 and Conv 5 has 512 filters. Three Fully-Connected (FC) layers follow a stack of convolutional layers: the first two have 4096

channels each, and the third performs 1000-way ILSVRC classification and thus contains 1000 channels (one for each class). The final layer is the soft-max layer. The input to Conv 1 layer is of fixed size 224 x 224 RGB image. To apply transfer learning, the dense layer was replaced with three dense layers of dimension 256 x 128 with ReLu activation and finally 1 sigmoid activation for binary classification. ModelCheckpoint callback was used to save the model if the validation accuracy of the model in the current epoch is greater than what it was in the last epoch. Earlystopping callback was used to stop the model's training early if there was no increase in parameter. Epoch was set to 100, and the patience was set to 20, which means that the model will stop training if there was no rise invalidation in 20 epochs. The model was evaluated, and the model with the best accuracy was validated (Mohan, 2020).

On the second experiment, the images from the inducing pseudopregnancy experiment, which data had been confirmed by the presence of a vaginal plug, were used. The images were cropped into a smaller size and only focused on the vulva of the vagina. The picture size was 600 pixels x 600 pixels and the resolution of 180 pixels/inch. The processing process was the same. By cropping the image, I hope to increase the system's accuracy. The number of samples are no plug n=125 and plug n=125. Ratio data training:test: 60:40, 70:30, and 80:20.

2.8.Statistical analysis

Quantitative data are presented as the means ± SEMs. The plug, pregnancy, and survival rates were analyzed using Fisher's exact test, with probability of $P<0.05$ was considered statistically significant. Pregnancy length, litter size, and body weight were analyzed using Kruskal-Wallis followed by Bonferroni correction, with probability of $P<0.05$ was considered statistically significant.

.

Chapter 3 - Result

3.1. Assessment of mouse estrous cycle

3.1.1. Visual examination of the mouse vagina

First, the vagina's appearance was examined by visual examination method. Female mouse morphology or appearance of the external part of genitalia was different at each stage (Champlin et al., 1973), as shown in table 2. In proestrus (Figure 3.1.A), the vaginal opening had a big gap, and the tissues appeared pink. Striation could be observed in both ventral and dorsal lips of the vulva of the vagina. Interestingly, the vagina color was found reddish during the estrus stage (Figure 3.1.B.). The striation became more prominent on estrus, as described by Champlin (Champlin et al., 1973). In the metestrus stage, the vagina color was pale (Figure 3.1.C), while in diestrus, the vagina color turned bluish (Figure 3.1.D).

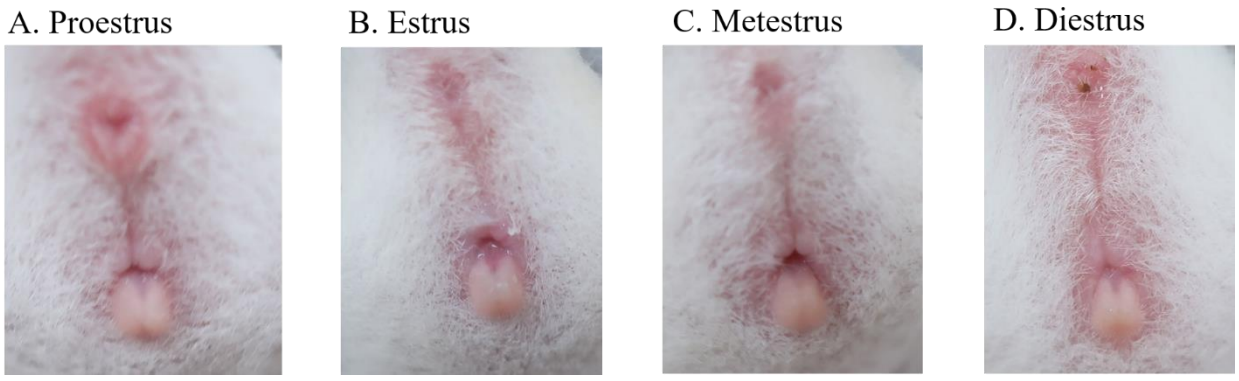

Figure 3.1. Four stages of the estrous cycle in ICR female mice. The four stages of the estrous cycle are shown based on vagina appearance for female ICR mice albino ICR strain: A. proestrus (P), B. estrus (E), C. metestrus (M), D diestrus (D).

3.1.2. Modification of Byers' vagina cytological examination method

Next, the reproducibility of the vagina cytological examination method was examined. At the beginning of the experiment, the method suggested by Byers et al. (2012, Figure 3.2.A.) was applied to obtain the vaginal cells. Byers acquired the vaginal cells by collecting them using a wet cotton-tipped swab and then introduced them into the vagina. The swab was turned and rolled gently against the vaginal wall and then removed. Cells on the cotton-tipped were transferred to a dry glass slide by rolling the swab on the glass slide. Figure 3.3.A. and 3.3.B. are glass slide observations from vaginal cells from the same mouse taken simultaneously, but from these slides, Figure 3.3.A. shows proestrus while figure 3.3.B. shows diestrus.

This result shows that Byers' method was not suitable for this study since many neutrophils were found left on the cotton swab cannot be transferred to the glass slide (Figure 3.3.A and C). The presence of neutrophils was very important in the vaginal cytology method since the proportion, presence, and absence of neutrophils is a must to be considered in deciding stages of the estrous cycle (Allen, 1922; Byers et al., 2012; McLean et al., 2012; Cora et al., 2015). Thus, the Byers method was modified by dipping the wet cotton-tipped swab into 25 µl PBS to catch and collect all the cell types before they were transferred into dry glass slides (Figure 3.2.B.). Through this modification, all three cell types: epithelial cell, cornified epithelial cell, and neutrophil, could be observed (Figure 3.3. B and D). Byers also air-dried the glass slide before stained the glass slide. This step was modified by drying the glass slide on the top of a warm bed or oven with a temperature of 56°C. With this drying method, the drying process was faster, and no neutrophils were ruptured (Figure 3.3. B and D).

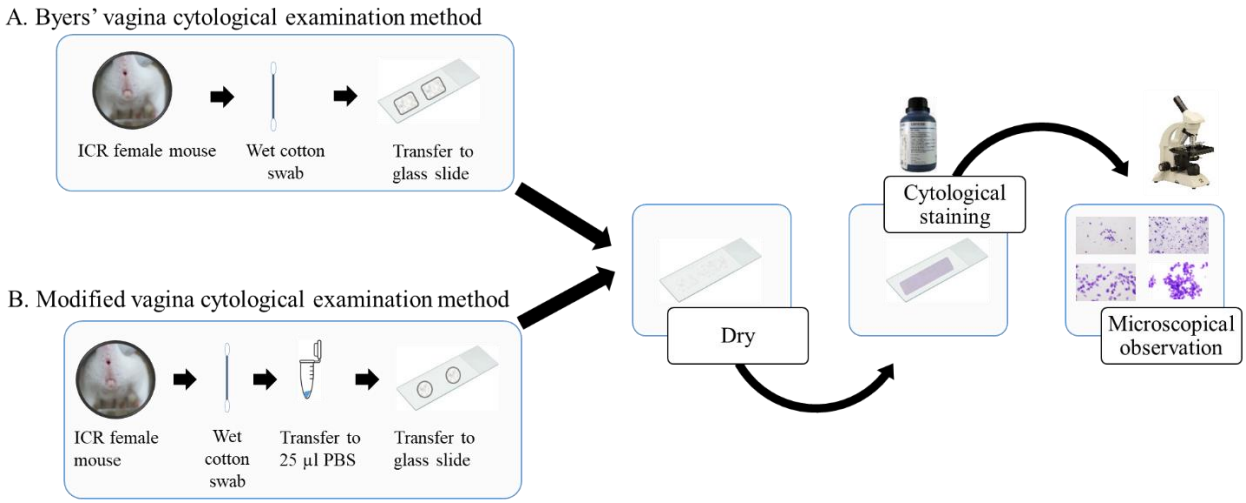

Figure 3.2. Modification of Byers' vagina cytological examination method. Modification of Byers' method (A) was done on the first step, Byers' transferred the cells directly to glass slide while on modified method (B), the cells were collected on microtube before transferred into glass slide.

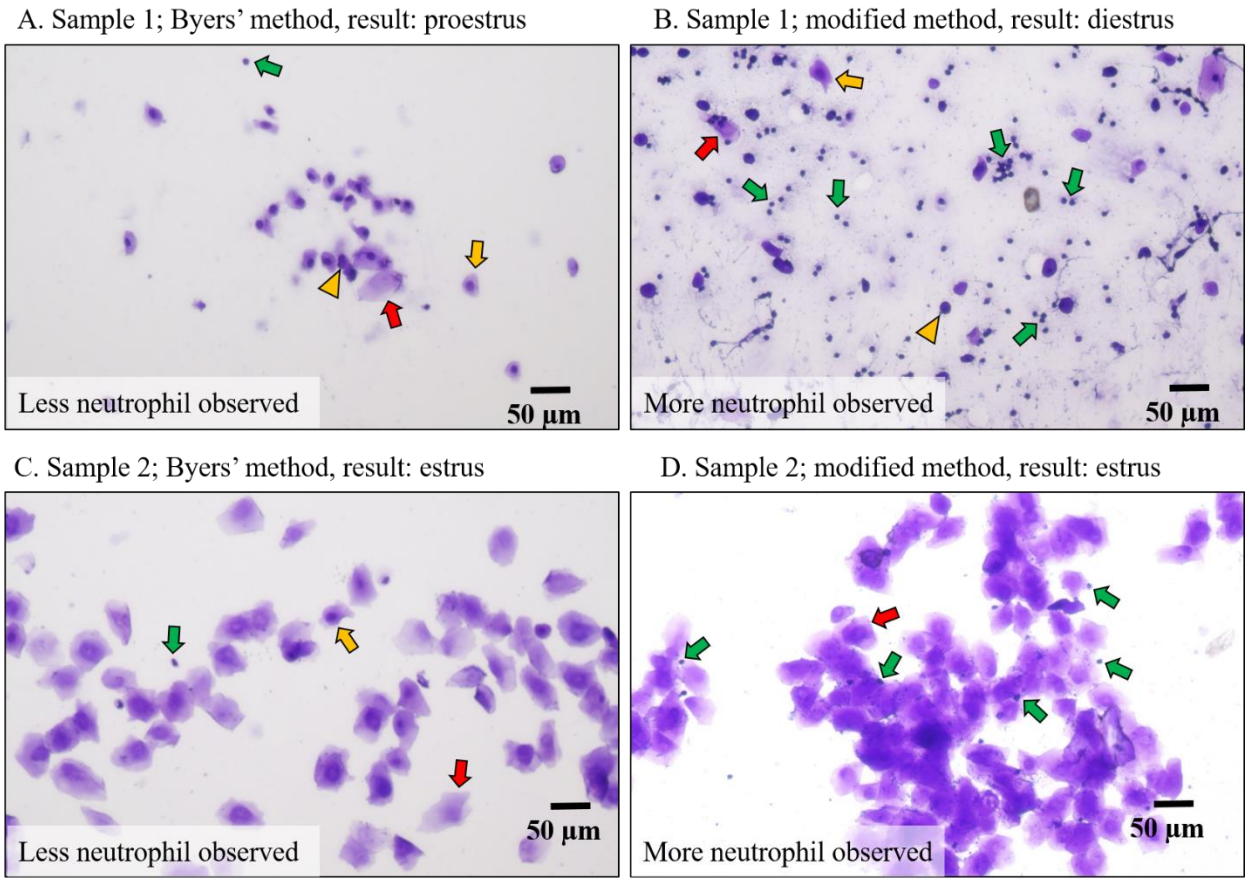

Figure 3.3. Modification of Byers's vaginal cytology method. By modified the Byers' vaginal cytology method, all cell types can be transferred to the glass slide (B, D). Byers's method failed to catch the neutrophils (A, C) but able to catch nucleated epithelial cells (A) and cornified epithelial cells (C). The green arrow is neutrophils, the yellow arrow is large nucleated epithelial cell, the yellow arrow head is small nucleated epithelial cell, the red arrow is cornified epithelial cell.

3.1.3. Vagina cytological examination method

Next, the estrous cycle of the mouse was examined by vagina cytological examination. Each estrus stage was characterized based on proportion, absence, and presence of the described three basic cell types as well as cell density and arrangement of the cells on the slides as explained in section 1.4.2., Figure 1.2., and Table 1.3. The proestrus stage was dominated by nucleated epithelial cells, while in the estrus stage, the observation was dominated by cornified epithelial cells, as shown in figure 3.4.A. The metestrus stages showed a mixture of all three cell types, but cornified epithelial cells and neutrophils were dominant, as shown in Figure 3.4.C. The diestrus stage showed a mixture of all cell types with neutrophils as the most significant proportion, as shown in Figure 3.4.D. During the progression of the estrous cycle, it was suggested that neutrophils aggregate during diestrus and then disappear with the onset of proestrus. During proestrus, nucleated epithelial cells appeared and were replaced by cornified epithelial cells when mice entered the estrus stage, as shown in Figure 3.4.B.

Females that are caged in a group setting (more than one mouse in one cage) might have longer or more irregular estrous cycle, which called “Lee-Boot effect” (Lee and Boot, 1955). To examine whether the Lee-Boot effect was happened to the mice that will be used on the study and as standard protocol to observe the status of the estrous cycle of mice in NAIST animal facility, 17 days of vaginal cells of six mice was collected with the modified Byers’ vaginal cytology examination method. The result is shown in Table 3.1.

The proestrus stage followed by the estrus stage (P-E) could be observed as shown in Table 3.1., in red. Since the normal estrous cycle for the mouse is 4-5 days, thus 3-4 cycles must be observed. During 17 days of observation, three proestrus stages followed by estrus (Table 3.1) can be observed. These mice and another extra 14 (total of 20) mice were used in the following experiment to collect vagina appearance digital images (photographs). The observation show that the result is not in sequences P-E-M-D during 4-5 days of observation, while Lee-Boot effect is happening, it doesn’t affect the normal cycle since the estrous cycle is cycling.

Table 3.1 Sample Data for Six Mice, Showing Their Estrous Cycle for 17 Consecutive Days[a]

ID	Day																	Number of days				No. of Cycles
	1	2	3	4	5	6	7	8	9	10	11	12	13	14	15	16	17	P	E	M	D	
1	M	D	D	E	D	D	P	E	M	D	P	E	D	P	E	M	P	4	4	3	6	3
2	D	D	D	P	E	M	D	P	E	M	D	P	E	E	M	D	P	4	4	3	6	3
3	P	E	E	M	D	D	P	E	M	D	D	D	D	D	P	E	E	3	5	2	7	3
4	E	M	D	D	D	P	E	M	D	P	E	M	D	P	E	M	D	3	4	4	6	3
5	D	D	P	E	E	M	D	D	P	E	D	P	E	M	D	D	D	3	4	2	8	3
6	D	P	E	M	D	D	D	P	E	D	P	E	E	M	D	D	D	3	4	2	8	3

[a] Abbreviation: P: proestrus; E: estrus; M: metestrus, D: diestrus

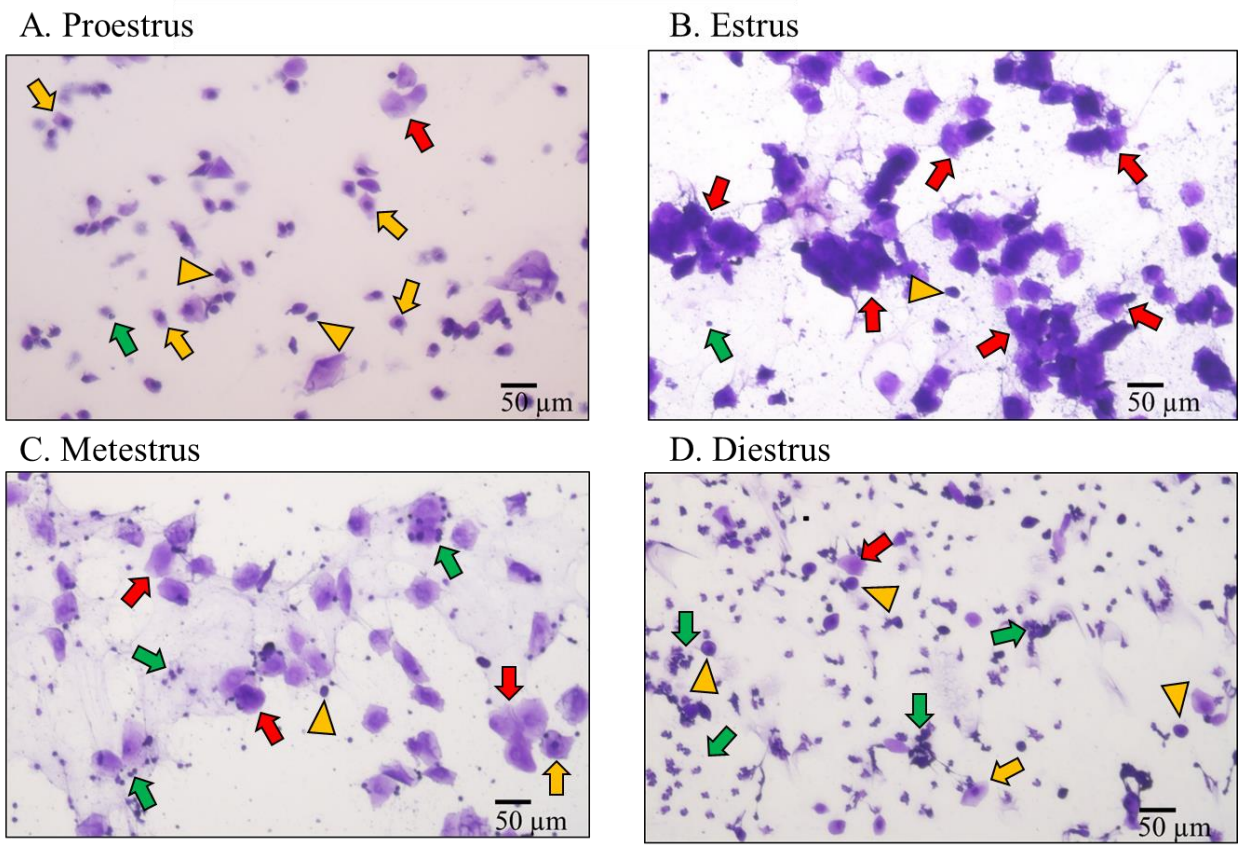

Figure 3.4. Vaginal cytology presenting each stage of the mouse estrous cycle. Four cell types are identified in vaginal smear images: neutrophils (green arrow), cornified epithelial cell (red arrow), large nucleated epithelial cells (yellow arrow), small nucleated epithelial cells (yellow arrowhead). Stages of the estrous cycle include: A. proestrus (P), B. estrus (E), C. metestrus (M), D. diestrus (D). The green arrow is neutrophils, the yellow arrow is large nucleated epithelial cell, the yellow arrow head is small nucleated epithelial cell, the red arrow is cornified epithelial cell.

3.2. Relationship between estrous cycle and successfulness in mating

3.2.1. Identification of vaginal plug in ICR female mice

Mouse in proestrus and estrus stages are in the most receptive condition when paired with male mice. Thus, pseudopregnant mice production rate will be the highest in those two stages. To understand the relationship between the estrous cycle and successfulness in mating, the female mice, which already know the estrous cycle, were paired with VAS mice. Pseudopregnant mice can be recognized by the vaginal plug presence (Figure 3.5.) that found in the next morning after being paired with male mice as a sign that mating or copulation was happening. The plug can be observed easily without blunt forceps as a plug with white (Figure 3.5.B.1.) to yellow color and sometimes red plug (Figure 3.5.B.1.) to brown. However, sometimes forceps need to be used to open the vagina opening to check if the plug has moved to the deep inside part of the vagina.

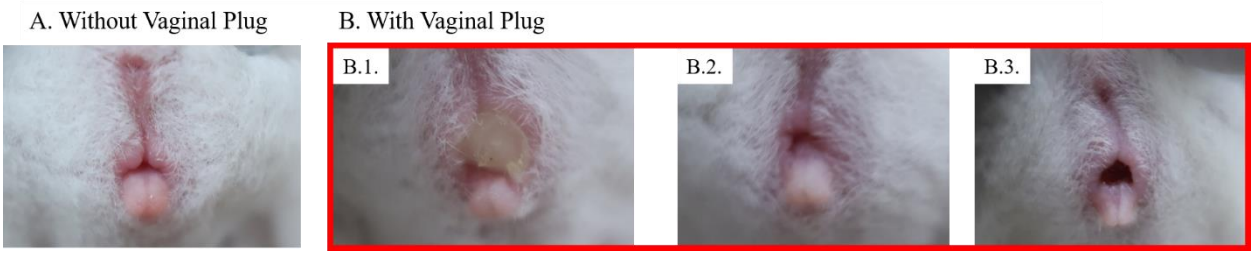

Figure 3.5. Vaginal plug in ICR female mice. Estrus mice (A) without plug after mating with VAS mice overnight compare to other mice which has plug after mating (B.1-3).

3.2.2. Vaginal Cytology Method on Production of Pseudopregnant Mice

From the total of 389 mice during the experiments, 53% was in receptive stages with 43% of them being in the estrus stage (Table 3.4.). Furthermore, 151 samples (39% of total data) were diestrus. The plug rate was shown in Figure 3.8.B. Both proestrus and estrus stages showed higher plug rates than metestrus and diestrus (Figure 3.8.B.), even though most of the mice selected were in estrus and diestrus stages (Figure 3.8.A.). Plug rate from proestrus and estrus stages were 64.1% and 63.9%, respectively, showing that successful mating and plug rate in proestrus and estrus stages are similar. Plug rate from metestrus and diestrus stages were 6.7% and 14%, respectively.

Table 3.2. Efficiency of Producing Pseudopregnant Mice Method by Assessing Estrous Cycle Using Vaginal Cytology Method

Estrous Cycle	No. (%) of females			Plug rate (%) ※
	No. pairing#1	With plug#2	Without plug#3	
Proestrus	39 (10)	25 (6)	14 (4)	64.10
Estrus	169 (43)	108 (28)	61 (16)	63.90
Metestrus	30 (8)	2 (1)	28 (1)	6.67
Diestrus	151 (39)	21 (5)	130 (33)	13.91
n total = 389				

#1 No. pairing: number of female mice that paired with VAS mice after cytology examination.

#2 With plug: number of female mice with a vaginal plug after pairing (copulated succeed);

#3 Without plug: number of female mice without a vaginal plug after pairing (copulated failed)

※Plug rate = With plug/ No. pairing

Plug were checked the following day after pairing with VAS male.

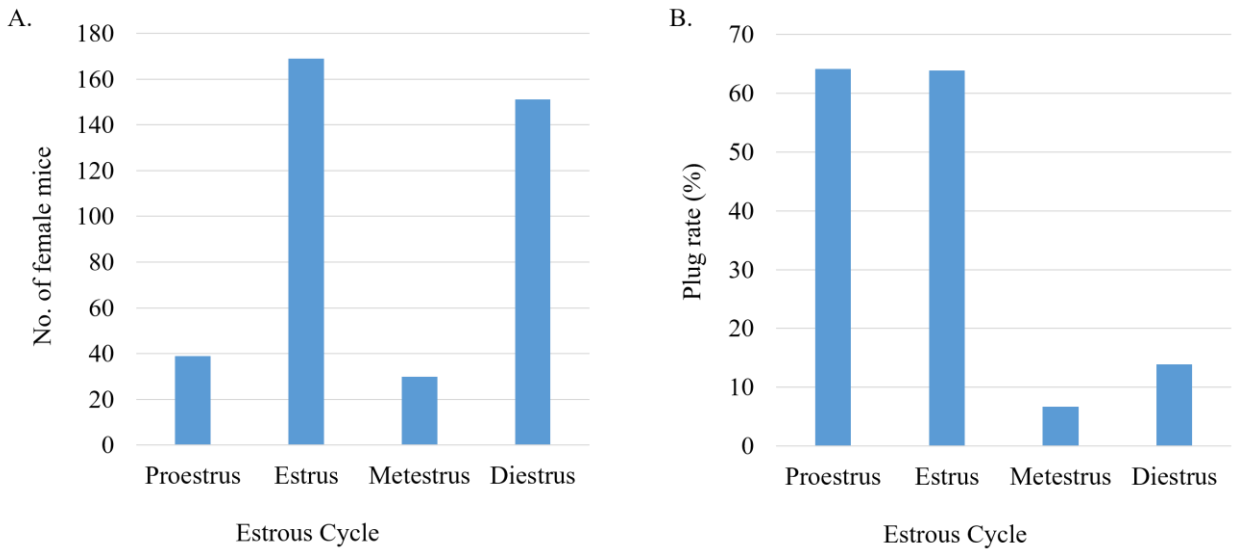

Figure 3.6. Vaginal plug rate from assessing estrous cycle using cytological method. Number of female mice on estrus and diestrus stages were dominated the assessment result (A), however, (B) plug rate % from total experiments showed that proestrus and estrus stages showed the highest success rate in mating.

3.3. Effect of the hormone treatment on estrus synchronization

3.3.1. Dose optimization of LHRHa to induce estrus on female mice

0.04 mg was the dose that has the ability to induce estrus on rats (Borjeson et al., 2014). To know if other dose might be more effective for mice, different dose of LHRHa were injected to mouse. After analyzing samples with vaginal cytological assay, LHRHa on dose 0.02 mg was synchronized estrus stage mice with the highest percentage (73%, Table 3.3., Figure 3.7.) comparing the other groups. Group 0.04 mg showed the lowest percentage of estrus stage (46.7%, Table 3.3., Figure 3.7.), while the lowest dose of 0.05 mg was the second highest estrus stage percentage (60%, Table 3.3., Figure 3.7.). However, all results of LHRHa treatment showed higher values compared to the control group. The control group was the mice randomly selected and not injected with any substances. No metestrus stage was observed at a dose of 0.005 mg and 0.04 mg (Figure 3.7.).

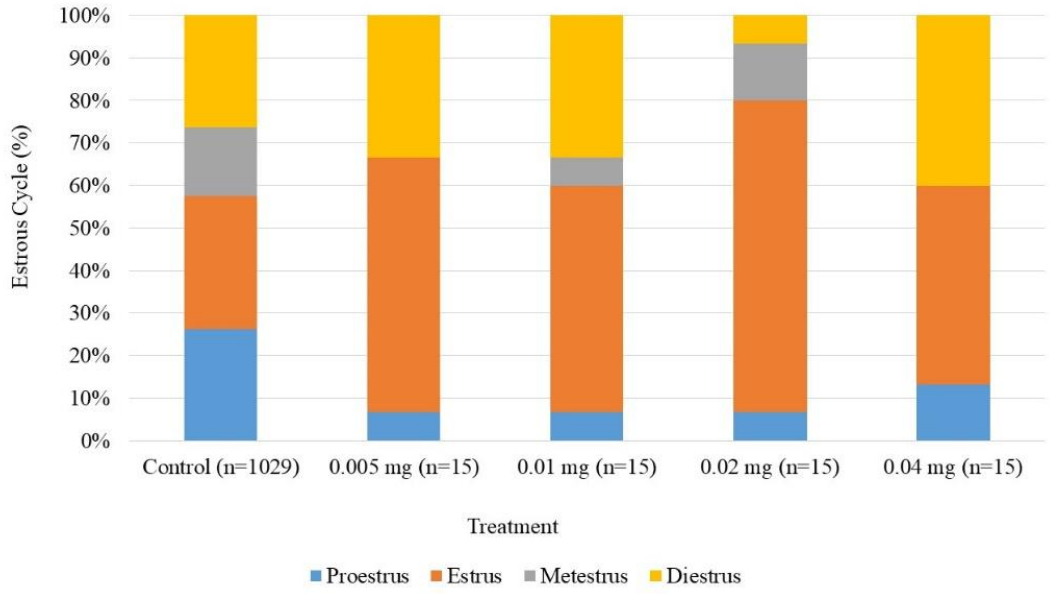

Figure 3.7. Effect of different dose of LHRHa treatment on ICR mice estrous cycle. All estrous cycle can be observed except for metestrus stage on dose 0.005 mg (lowest dose) and 0.04 mg (highest dose).

Table 3.3. Effect of different dose of LHRHa treatment on ICR mice estrous cycle

Treatment of LHRHa	n	No. (%) of females			
		Proestrus	Estrus	Metestrus	Diestrus
Control[#]	1029	220 (21)	264 (25)	136 (13)	409 (21)
0.005 mg	15	1 (6.7)	9 (60) *	0 (0)	5 (33.3)
0.01 mg	15	2 (6.7)	8 (53.3) *	1 (6.7)	5 (33.3)
0.02 mg	15	3 (6.7)	11 (73.3) *	2 (13.3)	1 (6.7)*
0.04 mg	15	2 (13.3)	7 (46.7)	0 (0)	6 (40)

*P<0.05 *vs* the corresponding value of the control, analyzed using Fisher's exact test. P-value detail is in supplementary 5.

[#] Female mice randomly choose and estrous cycle was judged by vagina cytological examination.

3.3.2. Effect of hormone treatment on the successfulness of mating

One strategy to get a high number of pseudopregnant mice is by preparing many proestrus-estrus stages on the pairing day. In this study, LHRHa was used to manipulate the hormone of the mice. Three different timing of injection, LHRHa_G1 (G1), LHRHa_G2 (G2), and LHRHa_G3 (G3), was performed to observe the effect of different timing or schedule of LHRHa administration (Table 2.1.). Mouse with LHRHa treatment successfully mated with the stud male ICR mice. Among LHRHa treatment, G1 showed the highest estrus rate (80%, Table 3.4., Figure 3.8.), similar to the PMSG treatment (Table 3.4., Figure 3.8.). G3 showed the second-highest estrus rate (66.7%, Table 3.4, Figure 3.8.) but also showed that with this treatment, some mice were synchronized in proestrus (13.3%, Table 3.4, Figure 3.8.), and when combined, the receptive stage of G3 is equal with G1 in 80% (Table 3.4, Figure 3.8.).

As hormone treatments have been reported previously, PMSG (Wei et al., 2015; Zhang et al., 2021) and progesterone (Hasegawa et al., 2017) showed successfulness in mating, with plug rate up to 100% for PMSG (Figure 3.9.A, Table 3.5.). Among LHRHa treatments, G3 shows the highest plug rate with 73.3%, followed by G1 with 40%, and the lowest was G2 with 30% (Figure 3.9.A., Table 3.5.). G1 and G2 showed a 100% pregnancy rate, while G3 showed 91% (Figure 3.9.B., Table 3.5.). All treatments showed no significant differences compared to the control for plug rate and pregnancy rate.

The normal pregnancy length for an ICR mouse is 19.5-20.5 days, Figure 3.9.C and Table 3.5. showed that all treatment has a normal length pregnancy day. G3 shows the smallest litter size among the LHRHa treatments compared to control (Figure 3.9.D, Table 3.5.). Body weight of the offspring from all LHRHa treatments showed no significantly difference from the controls.

The survival rate of all treatments, except for PMSG treatment ((P=0.00001, Fisher's exact test, $p<0.05$), were above 85% with G3 showed significant difference compared to control (P=0.0007, Fisher's exact test, $p<0.05$). G3's offspring shows a normal and healthy body after 24-hour observation. These results showed that G3 has potency as an established method to synchronize the estrous cycle in the estrus stage, and none of the LHRHa treatments affected embryonic development.

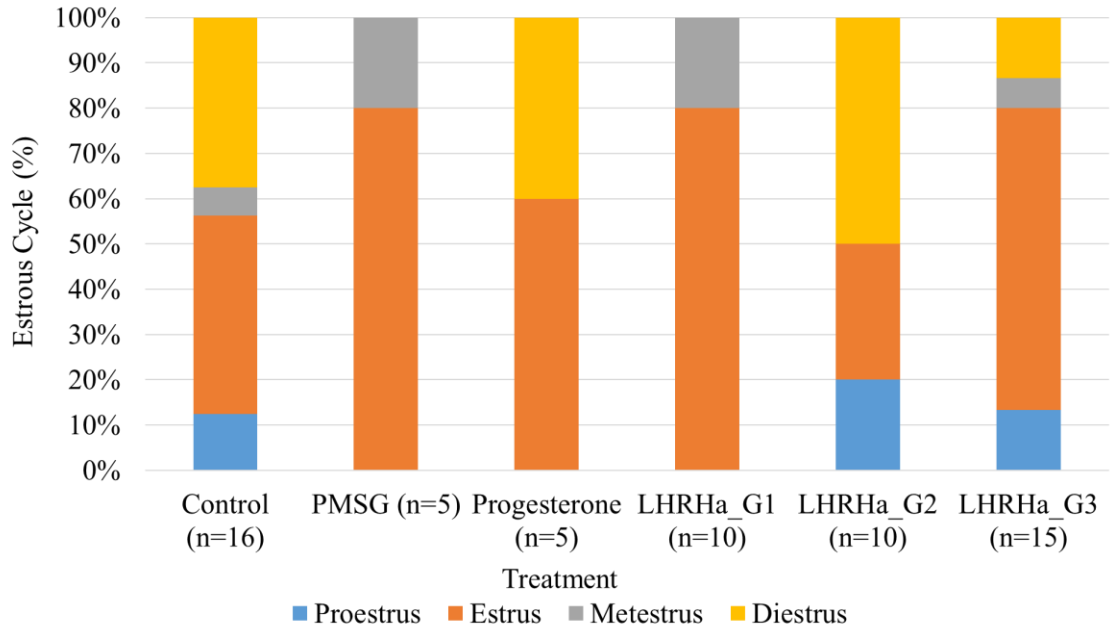

Figure 3.8. Effect of different hormone treatments on ICR mouse estrous cycle.

Table 3.4. Effect of different hormone treatment on ICR mice estrous cycle

Treatment	n	No. (%) Estrous Cycle			
		Proestrus	Estrus	Metestrus	Diestrus
Control[#]	16	2 (12.5)	7 (43.75)	1(6.25)	6 (37.5)
PMSG	5	0 (0)	4 (80)	1 (20)	0 (0)
Progesterone	5	1 (0)	3 (60)	0	2 (40)
LHRHa_G1	10	0 (0)	8 (80)	2 (20)	0 (0)
LHRHa_G2	10	2 (20)	3 (30)	0	5 (50)
LHRHa_G3	15	2 (13.3)	10(66.7)	1 (6.7)	2 (13.3)

[#] Female mice were selected by visual observation and followed by a cytological examination to confirm the estrous cycle.

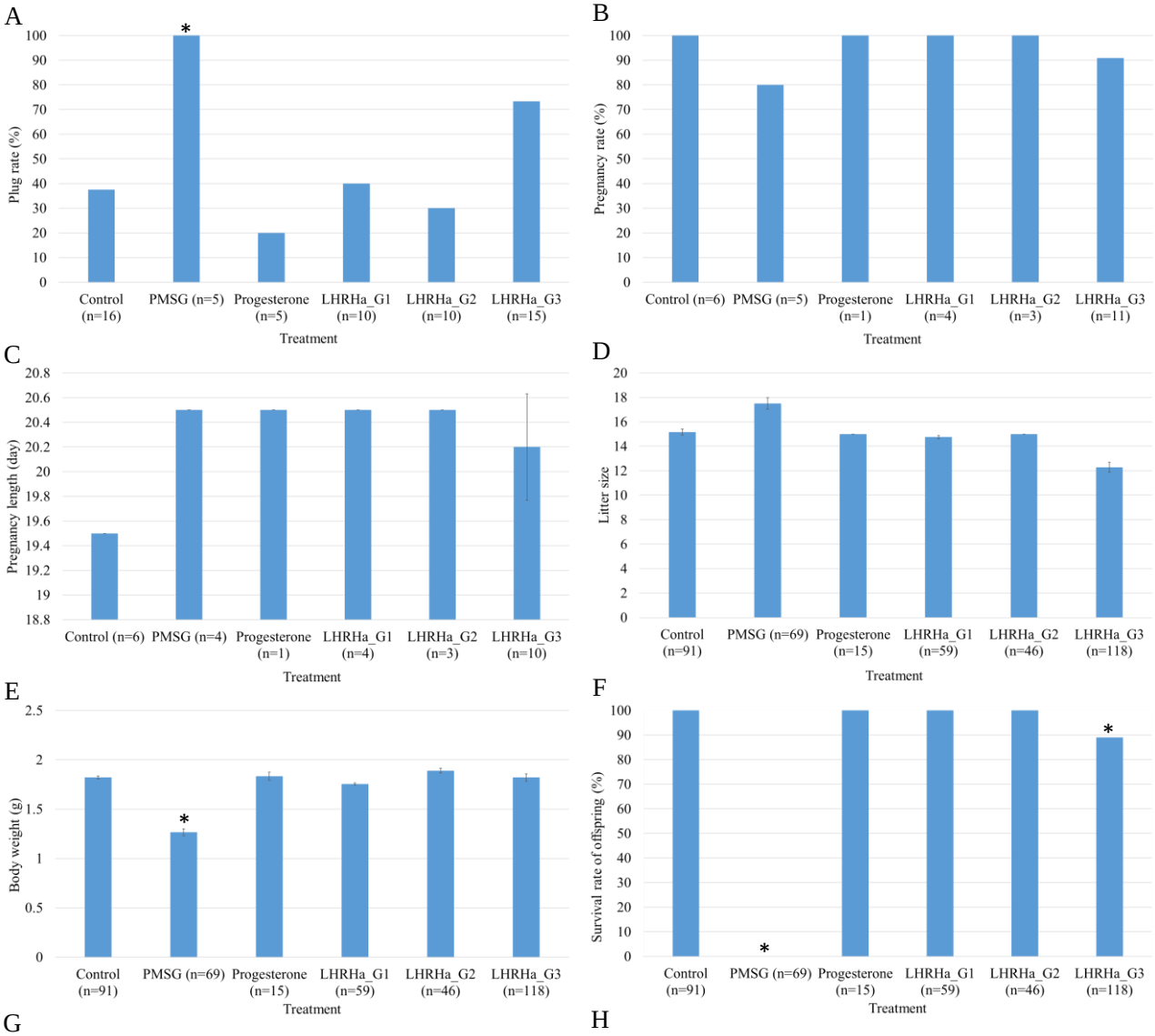
A
Plug rate (%)
Control (n=16)
PMSG (n=5)
Progesterone (n=5)
LHRHa_G1 (n=10)
LHRHa_G2 (n=10)
LHRHa_G3 (n=15)
Treatment
B
Pregnancy rate (%)
Control (n=6)
PMSG (n=5)
Progesterone (n=1)
LHRHa_G1 (n=4)
LHRHa_G2 (n=3)
LHRHa_G3 (n=11)
Treatment
C
Pregnancy length (day)
Control (n=6)
PMSG (n=4)
Progesterone (n=1)
LHRHa_G1 (n=4)
LHRHa_G2 (n=3)
LHRHa_G3 (n=10)
Treatment
D
Litter size
Control (n=91)
PMSG (n=69)
Progesterone (n=15)
LHRHa_G1 (n=59)
LHRHa_G2 (n=46)
LHRHa_G3 (n=118)
Treatment
E
Body weight (g)
Control (n=91)
PMSG (n=69)
Progesterone (n=15)
LHRHa_G1 (n=59)
LHRHa_G2 (n=46)
LHRHa_G3 (n=118)
Treatment
F
Survival rate of offspring (%)
Control (n=91)
PMSG (n=69)
Progesterone (n=15)
LHRHa_G1 (n=59)
LHRHa_G2 (n=46)
LHRHa_G3 (n=118)
Treatment
G
H
1.5 cm

Figure 3.9. Effect of difference hormone treatment embryo development. (A.) Plug rate (%) of PMSG are the highest and G3 the second highest, (B.) Pregnancy rate (%) of G1 and G2 were the highest with 100% rate, (C.) Gestation (day) of each group were varies but all of them were in normal gestating length of mouse (18-22 days), (D.) Litter size of G3 and Control groups were the lowest, (E.) Offsprings' body weight (g) of PMSG group was the lowest, (F.) Offsprings' survival rate (%) of PMSG was 0% while the other groups were 100% or almost 100%. (G) mother and pups from group G3. (H) pups (alive) from group G3. *$P < 0.05$ vs. the corresponding value of the control. Fisher's exact probability test was used in A, B, and F. Kruskal-Wallis test with Bonferroni correction was used in C, D, E.

Table 3.5. Effect of hormone treatment on the production of pseudopregnant mice and embryonic development to produce offspring

Experimental group	No. (%) of females		Pregnancy Length (day) [#2]	Litter size [#2]	No. of the offsprings [#2]	Body weight of the offspring (g) [#3]	Survival rate of the offspring (%)
	With plug [#1]	Pregnant					
Control	6/16 (37.5)	6/6 (100)	19.5 ± 0	15.1 ± 2.31	91	1.75 ± 0.17	91/91 (100)
PMSG	5/5 (100) *	4/5 (80)	20.5 ± 0	17.5 ± 3.87	69	1.32 ± 0.28*	69/69 (0)*
Progesterone	1/5 (20)	1/1 (100)	20.5 ± 0	15 ± 0	15	1.83 ± 0.15	15/15 (100)
LHRH_G1	4/10 (40)	4/4 (100)	20.5 ± 0	14.75 ± 0.12	59	1.74 ± 0.10	59/59 (100)
LHRH_G2	3/10 (30)	3/3 (100)	20.5 ± 0	15 ± 0	46	1.97 ± 0.14	46/46 (100)
LHRH_G3	11/15 (73.3)	10/11 (91)	20.2 ± 0.432	12.28 ± 0.411	105	1.92 ± 0.23	105/118 (89)*

[#1] Plug were checked the following day after pairing with VAS male.
[#2] n: All pregnant females in each experimental group
[#3] n: All offspring in each experimental group.
Data were presented as the means ± SEMs

*P < 0.05 vs. the corresponding value of the control. Fisher's exact probability test used in plug rate, pregnancy rate, and survival rate of the offspring. Kruskal-Wallis test with Bonferroni correction used in pregnancy length, litter size, and number bodyweight of the offspring.

3.4. Machine learning approach

3.4.1. Data collection and estrous cycle assessment

A total of 1040 pictures of digital images of vagina appearance and cytological assessment result were collected during 2020 as shown on table. Two examiners, examiner I and examiner 2 did the cytological assessment to determine the estrus stages of the mouse (Table 3.6., Figure 3.10.A-B.). From 1040 cytological samples, only 579 samples (55.7%) that agreed on the same stage of estrus by both examiners as shown on figure 3.5.B. while the percentage of estrous cycle were almost similar (Figure 3.10. A-B.). Number of samples identified that matched, used as the control for estrus or receptive stages (proestrus-estrus) as random selection in the next experiments. In addition, for a total of 373 specimens, the two examiners disagreed in determining the stages of proestrus and estrus for a total of 83 samples and metestrus and diestrus for a total of 91 samples. Distribution of each stage: proestrus, estrus, metestrus, diestrus is not evenly with the highest proportion on diestrus and the lowest on metestrus (Table 3.6.).

Table 3.6. Identification of estrous cycle based on vaginal cell observation.

Estrous cycle	No. (%) of data		
	Examiner 1	Examiner 2	Matched
Proestrus	186 (18)	254 (24)	119
Estrus	270 (26)	258 (25)	190
Metestrus	124 (12)	148 (14)	59
Diestrus	460 (44)	357 (34)	299
Not determined		23 (2)	

n total = 1040

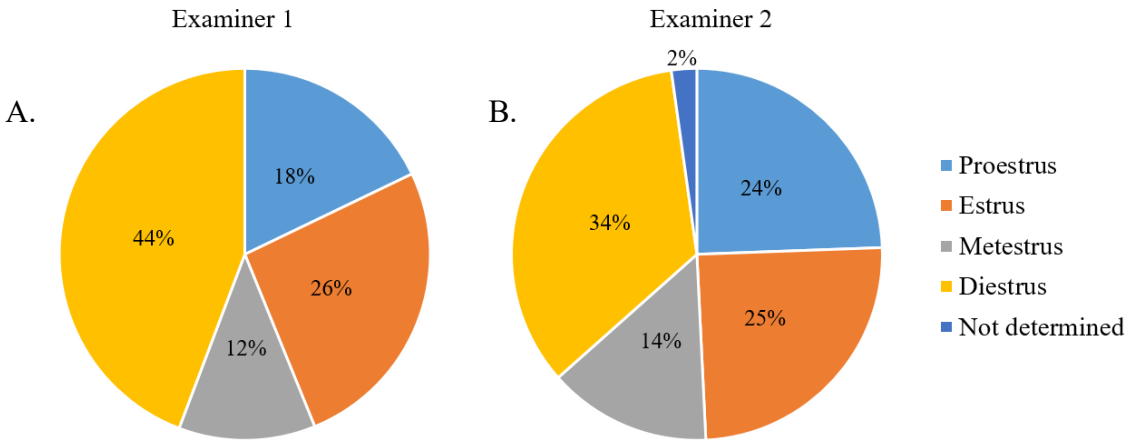

Figure 3.10. Subjectivity among two examiners. Examiners 1 (A) and examiner 2 (B) showed different assessment result for vaginal cytology observation.

3.4.2. Development of machine learning using digital images of vagina appearance

The machine learning system built to classify the receptive stages (proestrus-estrus) and non-receptive stages (metestrus-diestrus) as shown in Figure 3.11.A. Images with original size were used on this experiment. From all experiments, by differentiating the training and test, both the loss and the accuracy scores were bad because the loss score was high on the range of 0.6972 to 0.7001 and the accuracy was low in the range of 50.76 % to 44.44% (Table 3.7., Figure 3.11.B). Furthermore, Figure 3.11.B shows that the loss value is not decreasing but oscillating, which shows the model might not be learning at all.

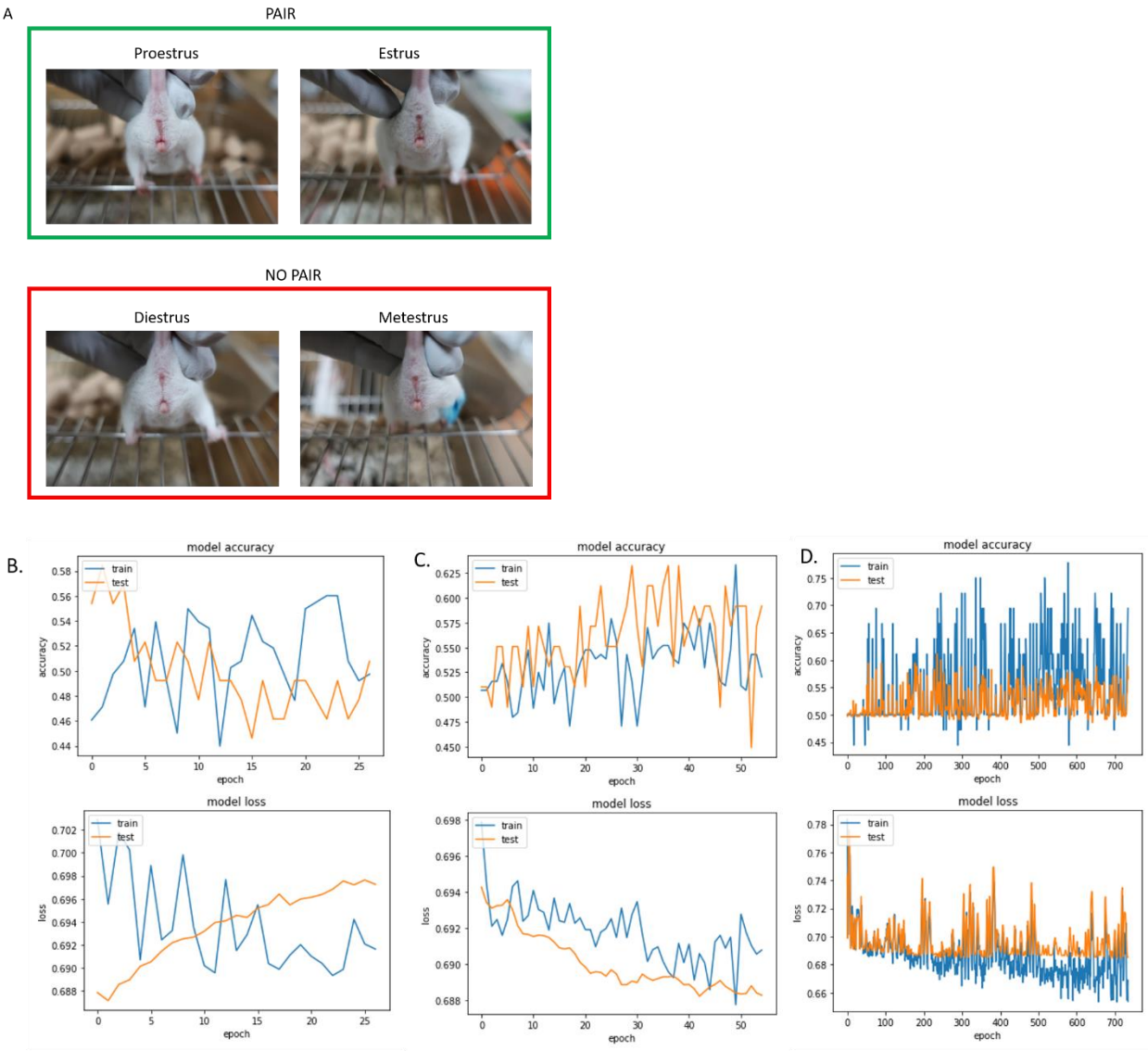

Figure 3.11. Classify the receptive and non-receptive stages of estrous cycle to decide the pairing or not. (A.) The PAIR class consists of vagina appearance from proestrus and estrus stages and NO PAIR class consists of metestrus and diestrus stages. (B). The model accuracy and loss plot for training:test = 60:40. (C). The model accuracy and loss plot for training:test = 70:30. (D). The model accuracy and loss plot for training:test = 80:20.

Table 3.7. Performance of machine learning on different training and test data ratio to classify receptive stages and non-receptive stages

Training	Test	Performance
60	40	Loss: 0.6972 Accuracy: 50.76% Remarks: early stopping on epoch 27/100
70	30	Loss: 0.6882 Accuracy: 59.18% Remarks: early stopping on epoch 55/100
80	20	Loss: 0.7001 Accuracy: 44.44% Remarks: early stopping on epoch 42/100

3.4.3. Implementation of machine learning on production of pseudopregnant mice

The machine learning system was built to classify the vagina appearance that has successful mating when paired (as PAIR class) with male mice and failed to mate (as NO PAIR class) as shown in figure 3.12.A. The resized image was used in this experiment. From all experiments, by differentiating the training and test ratio, the loss and the accuracy scores were bad because the loss score was high on the range of 0.6894 to 0.7006, and the accuracy was low in the range of 53.33 % to 49.71% (Tabel 3.8., Figure 3.12. B). Furthermore, Figure 3.12. B shows that the loss value is not decreasing, but it is just oscillating, which shows that the model might not be learning at all.

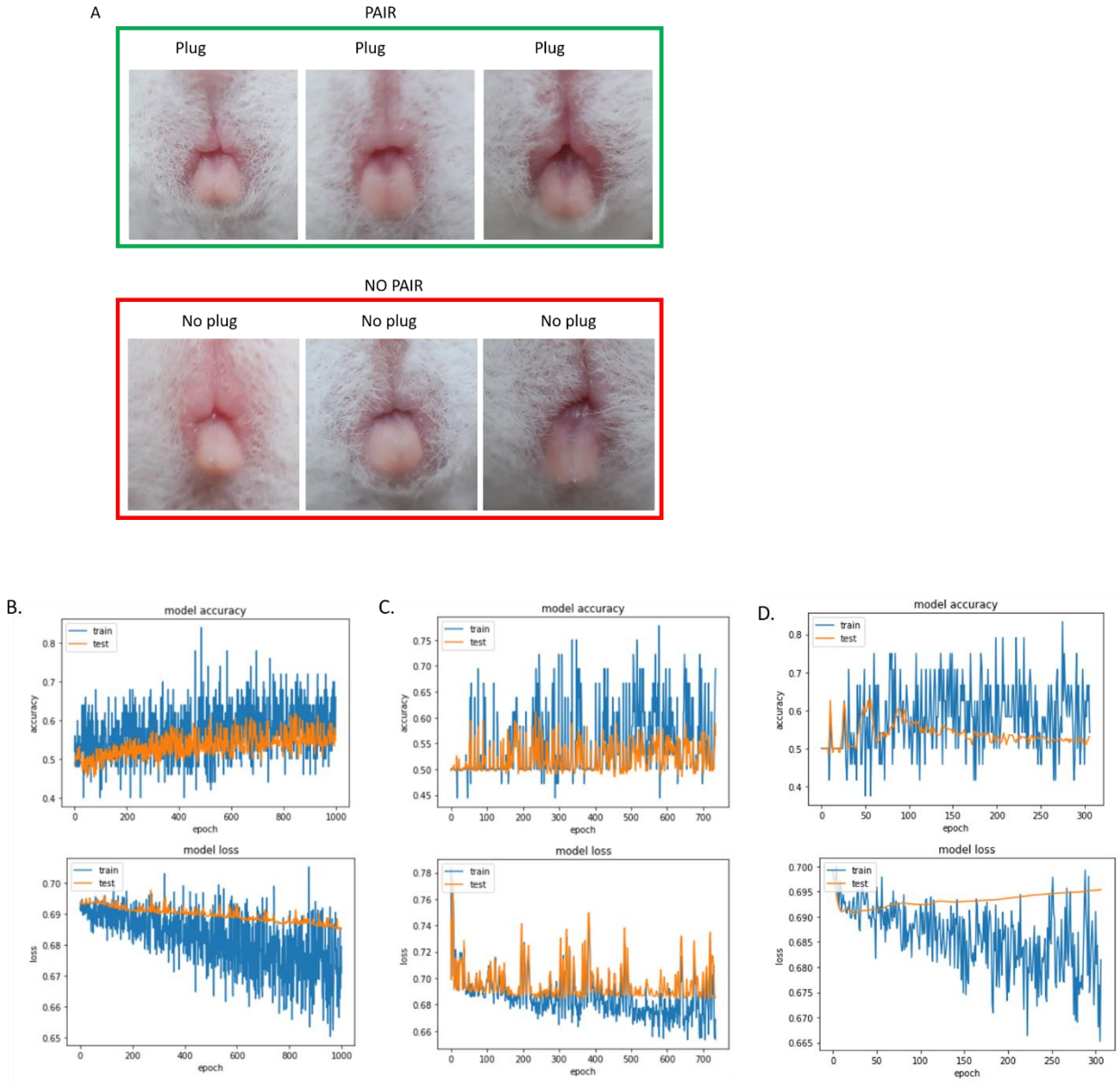

Figure 3.12. Classify the receptive and non-receptive stages of estrous cycle to decide the pairing or not. (A.) The PAIR class consists of vagina appearance with plug result and NO PAIR class consists of vagina appearance with no plug result. (B). The model accuracy and loss plot for training:test = 60:40. (C). The model accuracy and loss plot for training:test = 70:30. (D). The model accuracy and loss plot for training:test = 80:20.

Table 3.8. Performance of machine learning on different training and test data ratio to classify receptive stages and non-receptive stages

Training	Test/ Validation	Performance
60	20/20	Loss: 0.6894 Accuracy: 53.33% Remarks: complete epoch 1000/1000
70	15/15	Loss: 0.7006 Accuracy: 49.71% Remarks: early stopping on epoch 534/1000
80	10/10	Loss: 0.6932 Accuracy: 49.9% Remarks: early stopping on epoch 299/1000

Chapter 4 – Discussion

4.1. Cytological method for assessing the estrous cycle of mouse

The cytological examination method by collecting vaginal cells of the female mice and transferring them to a glass slide, staining, and then observing them under a microscope has been known as the most reliable technique in the detection of rodents' estrous cycle, including mouse (Cora et al., 2015). Three cell types: neutrophils, cornified epithelial cells, nucleated epithelial cells (in small and large size) can be observed during the experiments (Figure 3.4).

In this study, the vagina cells was obtained by using the swabbing technique. There are several methods to take the vaginal cells: washing the vagina orifice with pipetting, scrapping the dorsal vaginal wall (Emmens, 1950), and swabbing the vaginal walls (Byers et al., 2012). Collecting the vagina cells through the vaginal lavage by washing the vagina orifice using pipetting technique has weakness since this method only takes the sloughed cells. The results will be slightly delayed identification from the true stage of the estrous cycle since the sloughed cells are mostly from the previous day (Champlin et al., 1973). The two latter methods, scrapping and swabbing, are considered the better technique for taking the vaginal cells because cells from the wall epithelium can be obtained (Champlin et al., 1973).

Byers et al. (2012) reported the vaginal cytology method by swabbing technique and then transferring the cells on the cotton swab immediately to the glass slide. However, transferring the cells directly to the glass slide was not working in my study since the neutrophils failed to be transferred to the glass slide. To solve this problem, cells was transferred from the cotton swab to the 25 µl of PBS in a microtube. The PBS helped the cells that attached to the cotton swab to release and can be safely transferred to the glass slide without any sign of neutrophils rupture. Since the sample was on PBS liquid, different from Byers' method, the glass slide was dried on an oven or warm bed with a temperature of 56°C. By this heating method, the cell shapes can be maintained, and neutrophils are not ruptured. Neutrophils will rupture because of mechanical stress, such as being pressed into the glass slide (Guthrie, 2008). In this experiment, crystal violet was used to stain the cells; however, other metachromatic stains may be used to stain the dry fixed slides. Other slides that are commonly used to stain vaginal cells are Romanowsky-type stains and Toluidine blue O (Cora et al., 2015).

To do observation on estrous cycle, it is mandatory to check the status of the estrous cycle of the mice as an experimental animal in the study. Female mouse normally has a 4-5 days estrous

cycle when the female mice are caged in groups. The Lee-Boot effect is a condition when the estrous cycle of female mice is suppressed or prolonged because of the effect of an estrogen-dependent pheromone, possibly 2,5-dimethylpyrazine, which is released via the urine and acts on the vomeronasal organ of recipients (Lee and Boot, 1953). To check this condition in the NAIST animal facility, vaginal cytology samples for 17 consecutive days from the same mice was collected.

The samples were collected between 08:00-11:00 am. During 17 days of observation, the estrous cycle of all mice was found cycled three times. This showed that female mice in the NAIST animal facility have an approximately 5.7-day estrous cycle. While this day seems longer than the average regular 4-5 days estrous cycle (Byers et al., 2012; Cora et al., 2015), Nelson (Nelson et al., 1982) reported that a mouse has a longer estrous cycle, the next estrous cycle will be shorter. For example, a 5-days cycle will be followed by a 4-days cycle. This phenomenon can be observed clearly in mouse ID 6 (Table 3.2.), when the first P-E is found on day 3-4, then the second P-E is found on day 8-9 (5 days after the first P-E, long cycle), and then found again on day 11-12 (3 days after the first P-E, short cycle). Caligioni (2009) reported that the observation sequences were not always P-E-M-D. I also observed extra estrus and diestrus stages, which are normal to be observed in mice (Caligioni, 2009), probably due to the Lee-Boot effect. Therefore, the result showed that our mice were in normal estrous length, and the estrous cycle was normally cycling.

From vaginal cytology observation, diestrus samples dominated the sample collection process, and metestrus was the lowest number. This number correlates with the natural length of the estrous cycle. Diestrus is the longest stage where it can last up to 72 hours (Cora et al., 2015), so it is dominating the sample's number. Proestrus length can be up to 24 hours, and estrus length can be up to 48 hours, but on average is 14 hours (Byers et al., 2012. While metestrus length is usually from 8-24 hours, metestrus is known as the shortest among other estrus stages in mice (Cora et al., 2015).

In the earlier experiments, the sample collection time was 08:00-10:00 am, and the chances of finding the sample with the characteristic of two stages were high. Such transition stage samples increased subjectivity among the examiners. Thus, the number of matched samples is low, only 55.7% (Table 3.6.). The proestrus sample was the second lowest after the metestrus sample. Proestrus is also a short stage like metestrus, and it usually does not appear until mid-morning. It was advisable to take samples between 10:00 am – 01:00 pm (OECD, 2008). Thus, the sample

collection time was prolonged to 11:00 am. While the method of deciding the estrous cycle by vaginal cytology has been known and established since 1922 (Allen, 1992), many aspects need to be considered by the experimenter so that the observation result is accurate and reliable in deciding the estrous cycle. While some aspects must be considered when applying the vagina cytological examination: a technique to obtain the vagina cells and the timing to take the vagina cells, therefore, vagina cytological examination technique is reliable to differentiate estrous cycle on mice.

4.2. Efficiency of preparing pseudopregnant mice by using the cytological examination method

Champlin has reported mouse vagina examination to differentiate the estrous cycle since 1973; however, the visual method of observing the appearance of the vagina still becomes obstacles in producing pseudopregnant mice. One reason is that an experienced and skillful experimenter was needed to make the assessment (Hasegawa et al., 2017). The visual method is not only faster and less stressful for the animals. It also can avoid the possibility of danger associated with mechanical manipulation of the vaginal tissue. There is a possibility that the inexperienced experimenter will stress or hurt the mouse by turning and rolling the cotton swab too fast or too harsh rather than gently as suggested by Byers' protocol vaginal cytology method when collecting the vagina cells (Byers et al., 2012). By using the visual method, bacterial transfer, vaginal secretion transfer, and pheromones among the animals can also be eliminated (Champlin et al., 1973).

While many reports (Champlin et al., 1973; Byers, 2012, Hasegawa et al., 2017; Ekambaram, 2017; Ajayi and Akhigbe, 2020) keep mentioning that the visual method technique needs an experienced and skillful experimenter, this technique is still useful to increase the efficiency in producing pseudopregnant mice. By using the vagina cytology method to decide the receptive mice, the plug rate was increased to 64.1% for proestrus and 63.9% for estrus mice. Inyawilert et al. (2016) reported that plug rate (%) mouse on proestrus and estrus stages up to 78.57% and 72.73%, respectively. Similar with Inyawilert et al. (2016), this study showed that proestrus and estrus are the receptive stages where the highest chances for mating is probably to happen.

4.3. Effect of the hormone treatment on estrus synchronization

Hormonal products can synchronized the estrous cycle of natural mating or artificial insemination which can increase the reproductive performance of animals (Wei et al., 2015). In this study, whether the pseudopregnant or pregnant females could be efficiently produced by synchronizing their estrous cycle was investigated. ICR female mice was used because this strain is frequently used as recipients in embryo transfer and as foster mothers after the Caesarian section. In this study, the female mice were paired with ICR intact males to collect the information about the offspring after hormone manipulation. Efficacy of progesterone in inducing estrus has been reported by Hasegawa (Hasegawa et al., 2017), and efficacy of PMSG was reported by Wei (Zhang et al., 2021). LHRHa has been known to have efficacy in inducing estrus in rats (Borjeson et al., 2014), but the efficacy on the mouse has not been known yet. LHRHa is a synthetic analog of GnRH (gonadotropin releasing hormone), a neurohormone that produce in the hypothalamus, and functions at the GnRH receptor, causing the release of FSH and LH from the anterior pituitary (Fink 1979).

First, the effect of different dosages of LHRHa in mice was observed to determine the optimal dose of the LHRHa treatment in inducing proestrus and estrus as receptive stages. In the result, the 0.02 mg LHRHa/mouse dose had highly synchronized the estrus stage. Interestingly, the highest dose of 0.04 mg, which is the same dose in rats, gave a lower percentage in producing proestrus-estrus mice. It is possible that on a higher dose, LHRHa inhibits the production of estrogen, thus ovulation cannot be started. LHRHa mechanism of action is based on the inhibition of pituitary and gonadal function (Schally, 1999). Chronic administration of LHRHa decreased the ovarian and uterine weights, reduced the concentration of plasma estradiol and progesterone, and produced various antifertility effects (Schally, 1994; Emons and Schally, 1994; Schally, 1999). This result summarizes that the dose 0.02 mg LHRHa/mouse is the best dose to induce the estrus stage in female mice. Progesterone group on this study showed a contrast result from Hasegawa et al. (2017), where the vagina plug rate with progesterone treatment reached up to 63%, but on this study only 20%. The difference might be related to the period of pairing between the male and female mice, Hasegawa et al. (2017) paired the mice for four days, while in this study, mice were paired for overnight and the vaginal plug was checked on the following day.

Next, after the hormone treatment, the female mice were paired with stud (WT) ICR males, and vaginal plugs were checked the next morning. Plug rate from the G3 (0.02 mg LHRHa/mouse treatment twice on a consecutive day) reached up 90%, higher than the plug rate by checking the estrous cycle using the vagina cytology. While the total dosage of this condition was 0.04 mg, the rate of the synchronization of estrous cycle was the highest of the experimental conditions. Some substances will be absorbed faster into the systemic circulation compared to the subcutaneous administration (Durk et al., 2018). Since, in this study, LHRHa was administrated through the intraperitoneal route, some of the LHRHa could be metabolized. By dividing the administration into two injections on two consecutive days, some LHRHa on the first day that may have been metabolized will be boosted by the second injection. As a result, this condition may have been synchronized the estrous cycle.

A vaginal plug can be observed around 8-24 hours after mating. Some plugs could be particularly thin and dissolve rapidly, especially when the males experience short periods of sexual rest (Sutter et al., 2016) or if the vaginal plug falls out (Behringer et al., 2016). The presence of a vaginal plug only indicated that copulation occurred but did not guarantee pregnancy (Behringer et al., 2016). This can be observed on one mouse in group G3 (this mouse was in proestrus stage) and one mouse from group PMSG (this mouse was estrus stage) as shown in Table 3.5. which has pregnancy rate less than 100%.

Mouse gestation (pregnancy) length is generally between 18-22 days (Murray et al., 2010). Thus the hormone treatment did not affect the length of gestation and most of the litter size. G3 showed a significantly different control of survival rate. The reason is that three mice in the group had extremely low litter pups, and those pups failed to survive during the 24-hour observation.

While pups which born from control, progesterone, G1, G2, and G3 were born healthy and safely, pups born from the PMSG group were attacked by the mother even though they were born alive. PMSG females ate the dead offspring and harmed the live-born pups since wounds could be observed on dead pups; this made all pups from the PMSG group fail to survive during 24 hours observation. This infanticide behavior is probably affected by PMSG treatment since all PMSG females killed their pups. Mann et al. (1983) reported that C57BL female mice exhibited infanticide behavior after hormone treatment (that injection of steroid hormone testosterone propionate and estradiol benzoate). Another possibility is that the PMSG mother had sensed the abnormality in the pups, so they killed them. Ovarian stimulation induced by PMSG in rodents is

associated with low birth weight (Zhang et al., 2021), thus PMSG group offspring bodyweight were the lowest among other groups and the survival rate was significantly different from the control group (Figure 3.12.E-F). Ovarian stimulation will decrease the level of progesterone and estrogen during pregnancy so that uterine natural killer cells fail to be regulated and affect the fetus's growth (Zhang et al., 2021). This abnormality might be the reason for the infanticide of PMSG female group.

Furthermore, when tetraploid complemented embryos were transferred to the pseudopregnant female from G3, more than 60% of offspring survived (Supplementary 3). This result summarizes that LHRHa administration with intraperitoneal injection technique, dose 0.02 mg, and injected twice in two consecutive days and then paired 72 hours later with the male mice (LHRHa 2x IP treatment): 1) induce estrus synchronization, 2) has highest rate of vaginal plug compared to the other LHRHa treatment, and 3) not affected the embryo development. Thus, this treatment could be proposed as new established method to produce pseudopregnant mouse.

4.4. Implementation of machine learning on producing of pseudopregnant mice

Machine learning was built as a potential solution for the need for experienced and skillful operators to decide on the proestrus-estrus stage in preparing the pseudopregnant mice. Just like its name, a machine learning system needs to learn so that the machine gains knowledge to do the classification. To do work properly, machine learning needs to learn from data, just like the experienced and skillful operator that has a lot of experience and training. Thus, data is the most important thing in building machine learning. In this study, the machine learning was developed based on VGG16 model, which has the ability to reach an accuracy of up to 92.7% (Simonyan and Zisserman, 2015).

In this study, the number of data samples was considered low, mainly because the image of the vagina's appearance has many similarities among the classes (estrous cycle). For example, to build a strong and accurate classification of cats and dogs, up to 97%, 25000 images of cats and dogs each were needed (Mohan, 2020). VGG16 (Supplementary 1) has been reported to succeed in classifying 17 flower species by only 80 images for each species, with an overall performance of 72.75% (Nilsback and Zimmerman, 2008).

Another strategy was tried by focusing on upper side striation and the vulva shape of the mouse vagina, and the system was designated to differentiate receptive stages (proestrus-estrus)

and non-receptive stages (metestrus-diestrus). However, this method also failed to increase the accuracy since the judgement result between machine and human examiner is lower compare than judgement of two examiners (Supplementary 2).

The failure of the machine learning system to have high accuracy in this study seems to happen because the data was not enough to train the machine to classify the estrous stages. To increase the number of data, the data between proestrus and estrus were combined. On this receptive stages, the vagina appearance has many similarities, such as on striation of vagina and opening of vagina. This group was named as 'pairing' group. Metestrus and diestrus were in the 'no pairing' group since these two stages have similarities in no swelling, no striation, the vagina tissues look paler, and small to the very small opening of the vagina. Unlike Nilsback and Zimmerman (Nilsback and Zimmerman, 2008) flower data that can be differentiated clearly from color, texture, and shape, features on vaginal appearance are more limited. In another comparison, Sano (Sano et al., 2020) succeeded in classifying (accuracy 93.3%) mouse estrous cycle by applying the VGG16 model to vaginal cytology slide observation with total samples of 2,096 microscopy images (P: n = 171, E: n = 449, D: n = 1,476). With low number of data on this study (total 938 images; P: n = 208, E: n = 362, M: n = 106, D: n = 482), it means not enough information for the machine to learn how to classify the object. This strategy and data availability are insufficient to build the machine learning system. This can also be seen from the loss of every machine learning experiment where the loss value is not decreasing but is only oscillating, which informs us that the model might not be learning. The number of data that I have become the biggest limitation to building the machine learning system. With this high loss and low accuracy, the system shows many errors when making the prediction.

Moreover, Champlin et al. (1973) stated that an untrained human observer could mistake for proestrus-estrus stages for late metestrus and diestrus since the vaginal tissues may be pink, but the opening has not yet returned to their smallest size. This reason could make the machine learning fail and the machine similar to the untrained human observer.

Chapter 5 –Conclusion

5.1. Conclusion

Production of pseudopregnant mice has been an inefficient process because it depends on the experience and skill of the observer. Furthermore, this embryo transfer step is relatively unchanged compared to other ART techniques. In this study, I made an effort to establish several approaches to be proposed as a method to increase efficiency in pseudopregnant mice production.

The machine learning approach failed to classify the receptive stages (proestrus and estrus stages) and non-receptive stages (metestrus and diestrus stages). The number of data becomes the limitation of this study to develop the machine learning system with high accuracy and low loss result.

In contrast with machine learning, the cytology method, established in 1922 (Allen, 1922), is still a strongly advisable method to differentiate the estrous cycle in mice. By collecting vaginal cytology data, I found that 21.1 % in proestrus, 25.5% in estrus, 13.1 % in metestrus, 39.3% in diestrus. This data correlates with the length of each stage of the estrous cycle; for example, since diestrus is the longest stage, the percentage ratio is the highest. With vaginal cytology, the vaginal plug rate from a mouse classified as proestrus and estrus stages is 64.1% and 63.9%, respectively, and metestrus and diestrus, 6.67% and 13.91%, respectively. By this information, I can expect that in colony of total 1000 mice, around 140 mice in proestrus stage, and around 160 mice in estrus stage, will have vaginal plug when mated with male (formula: expected mouse with plug rate without vaginal cytology = rate each stage * vaginal plug rate stage /100; example for proestrus: 21.1% * 64.1% / 100 = 13.5%). Thus, vaginal plug rate that can be obtained from each stage is P= 13.5%, E= 16.2%, M= 0.87%, D= 5.46%. Thus, the total expected of the vaginal plug is 36% by random selection. So that, with the random selection, we need to prepare a 3-4 times higher number of mice.

For the production of the pseudopregnant mouse, LHRHa_G3 (G3) or LHRHa 2x IP treatment can reduce the number of mice that needed up to 79% compared to the standard method by visual examination. For example, to prepare 10 pseudopregnant mice by visual examination, we need to choose at least 25 females on proestrus and estrus stages from a total of at least 67 female mice, then pair those 25 females mice with 25 VAS males. With LHRHa 2x IP treatment; this number can be reduced to 14 mice for each gender (Figure 5.1).

More extensive study is needed to expand the understanding of how LHRHa induces estrus synchronization in mice by considering their progesterone and estrogen level to maintain the development of the pup's growth as a surrogate mother in embryo transfer. The possibility of infanticide behavior is also needed to study because if the surrogate mother shows the infanticide behavior, GEMM pups will be killed by the mother during the birth, and the data experiments could not be obtained.

The result from this study will be useful not only for adding information about the function of LHRHa in mouse estrus synchronization but also will help many labs that especially work with the pseudopregnant mouse to save the space in their animal facility, reduce the cost of maintaining the mouse facility, and keep the spirit and principle of 3Rs – reduction, refinement, and replacement in animal experiment. Most importantly, this study also contributes to the advancement of artificial reproductive technology.

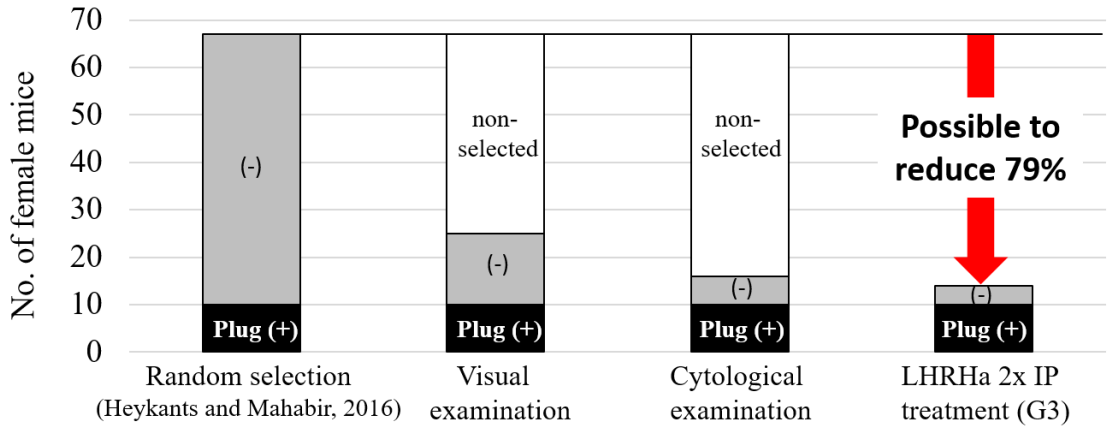

No. of Plug (+) female (efficiency)	10 mice (15%)	10 mice (40%)	10 mice (64%)	10 mice **(73%)**
No. of need female	67 mice	67 mice	67 mice	**14 mice**
No. of need male	67 mice	25 mice	16 mice	14 mice
Efforts for preparation		Training (long time)	Cytological analysis (>3 hr) + training	**IP injection (10 min x 2 days)**

Figure 5.1. Schematic representation of the number of a female mouse required for the production of the pseudopregnant mice.

Chapter 6 - Acknowledgment

First and foremost, I would like to express my sincere gratitude to my supervisor, Associate Professor Ayako Isotani, PhD for her unlimited support, encouragement, and patience throughout my studies. Her great knowledge and wisdom not only helped me in all the time of research and writing this thesis but also on my daily life. I could not complete my studies without her endless guidance and tireless effort. I also would like to thank Assistant Professor Shunsuke Yuri, PhD who always been open for discussion and being helpful during my study.

My sincere gratitude to my thesis committee: Prof. Yasumasa Bessho, PhD, Prof. Akira Kurisaki, PhD, and Prof Yuichi Sakumura, PhD, for their insightful, valuable critical advice, feedback, and support my research.

I am grateful to the Indonesian Government who supported my study through LPDP scholarship.

The biggest thanks and love to both of my parents and brother, who have been my main moral support from the beginning I have this crazy idea to do a study abroad until I finally completed my doctoral program. Thank you to my family and friends who have been constantly praying and wishing me the best to finish my study.

Thank you for Jekson, Harti, Mochi, Denise, Domon, Tamara and Yunki for the endless support and encouragement.

I would also like to thank my fellow labmates, from 2018 to recently, for their continuous support. My dearest labmates who have made working in the lab become a brightful day, Yamamoto-san, Nakano-san, Fujio-san, Kanatani-kun, Patrick, and Jon.

Next, I would like to express my deepest appreciation to Indonesian community and ADHD Indonesia Community. Special thanks to James, Brig, Asti, Anggun, Olla, Aghni, Ria, Aini, Rani, Beni, Diki, Lily, Dhania, and Indra who have helped me through thick and thin in Japan. And last, but not least, a huge gigantic thanks for my little Ms. Noisy, a girl who always push me to the edge and force me to take the leap. Yes! you are right, we are okay and we are ready to break some legs again.

Chapter 7 – References

Abate-Shen C, Pandolfi PP. Effective utilization and appropriate selection of genetically engineered mouse models for translational integration of mouse and human trials. Cold Spring Harbor Protocols. 2013 (11): 1006–11.

Achiraman S, Archunan G, Sankar Ganesh D, Rajagopal T, Rengarajan RL, Kokilavani P, Kamalakkannan S, Kannan S. Biochemical analysis of female mice urine with reference to endocrine function: a key tool for estrus detection. Zool Sci. 2011;28:600–5.

Agca Y. Genome resource banking of biomedically important laboratory animals. Theriogenology. 2012; 78: 1653–65.

Ajayi AF, Akhigbe RE. Staging of the estrous cycle and induction of estrus in experimental rodents: an update. Fertil Res and Pract. 2020;6:(5).

Allen E. The oestrous cycle in the mouse. Am J Anat. 1922; 30, 297–371.

Andreas Sutter, Leigh W. Simmons, Anna K. Lindholm, Renée C. Firman, Function of copulatory plugs in house mice: mating behavior and paternity outcomes of rival males. Behavioral Ecology. 2016; 27: 185–195.

Andrews WW, Ojeda SR. A detailed analysis of the serum LH secretory profiles of conscious free-moving female rats during the time of puberty. Endocrinology. 1981; 109:2032–9.

Archunan D, Dominic CJ. Oestrous cycle disruption in group-housed mice: evaluation of the involvement of tactile and pheromonal stimuli. Acta Physiol Hung. 1991; 78: 275-82.

Auta T, Hassan AT. Alteration in oestrus cycle and implantation in Mus musculus administered aqueous wood ash extract of Azadirachta indica (neem). Asian Pacific J Reproduction. 2016; 5(3):188–92.

Behringer R, Gertsenstein M, Nagy KV, Nagy A. Selecting female mice in estrus and checking plugs. Cold Spring Harb Protoc. 2016 Aug 1;2016(8).

Borjeson TM., Pang J, Fox JG, Garcia A. Administration of luteinizing hormone releasing hormone agonist for synchronization of estrus and generation of pseuopregnancy for embryo transfer in rats. J Am Assoc Lab Anim Sci. 2014 May; 53(3): 232–7.

Byers SL, Wiles MV, Dunn SL, Taft RA. Mouse estrous cycle identification tool and images. PLoS One. 2012;7(4):e35538.

Caligioni C. Assessing reproductive status/stages in mice. Curr Protoc Neurosci. 2009; Appendix 4I p. 1-6.

Champlin AK, Dorr DL, Gates AH. Determining the stage of the estrous cycle in the mouse by the appearance of the vagina. Biol Reprod. 1973;8(4):491–4.

Cora MC, Kooistra L, Travlos G. Vaginal cytology of the laboratory rat and mouse: review and criteria for the staging of the estrous cycle using stained vaginal smears. Toxicol Pathol. 2015;43:776–93.

Critser ES, Rutledge JJ, French LR. Effect of indomethacin on the interestrous interval of intact and hysterectomized pseudopregnant mice. Biol Reprod. 1981; 23: 1000-5.

Cunningham, James G.; Klein, Bradley G. Textbook of Veterinary Physiology (Fourth ed.). 2007. St. Louis: Elsevier Inc.

Corbin A, Bex FJ. Reproductive pharmacology of LHRH and agonists in females and males. Acta Eur Fertil. 1980 Jun;11(2):113-30.

Dewar AD. Body weight changes in mouse during the oestrus cycle and pseudopregnancy. J Endocrinol. 1957;15: 230-3.

Dewar AD. Effect of hysterectomy on corpus luteum activity in the cyclic, pseudopregnant and pregnant mouse. J Reprod Fertil. 1973; 33: 77-89.

Dewar AD. Observation on pseudopregnancy in the mouse. J Endocrinol. 1959; 18:186-90.

Durk MR, Desmukh G, Valle N, Ding X, Bianca M. Extravascular dosing in cassette brain microdialysis studies. Drug Metabolism and Disposition. 2018; 46(7): 964-9.

Dobson GP, Letson HL, Biros E, Morris J. Specific pathogen-free (SPF) animal status as a variable in biomedical research: Have we come full circle? EBioMedicine. 2019; 41:42-43.

Ehteshami BB, Veta M, Johannes van Diest P, van Ginneken B, Karssemeijer N, Litjens G, et al. Diagnostic assessment of deep learning algorithms for detection of lymph node metastases in women with breast cancer. JAMA. 2017; 318: 2199–210.

Emons G, Schally AV. The use of luteinizing hormone releasing hormone agonist and antagonist in gynecological cancers. Hum Reprod. 1994; 9: 1364-79.

Ericsson AC, Crim MJ, Franklin CL. A Brief History of Animal Modeling. Missouri Medicine. 2013; 110(3):200-5.

Esteva A, Kuprel B, Novoa RA, Ko J, Swetter SM, Blau HM, Thrun S. Dermatologist-level classifcation of skin cancer with deep neural networks. Nature. 2017; 542: 115–8.

Field, A. (2013) Discovering Statistics using SPSS: (And sex and drugs and rock 'n' roll). 4 th edn. London: SAGE.

Fink G. 1979. Feedback action of target hormones on hypothalamus and pituitary with special reference to gonadal steroids. Annu Rev Physiol 41: 571-85.

Freeman ME. The neuroendocrine control of the ovarian cycle of the rat. In: Knobil E, Neill JD, editors. The physiology of Reproduction. 2nd ed. New York: Raven Press; 1994.

Greenwald GS and Rothchild I. Formation and maintenanceof corpora lutea in laboraty animals. J Anim Sci. 1968; 27: Suppl 1: 139-62.

Hasegawa A, Mochida K, Ogonuki N, Hirose M, Tomishima T, Inoue K, Ogura A. Efficient and scheduled production of pseudopregnant female mice for embryo transfer by estrous cycle synchronization. Journal of reproduction and development, 2017; 63 (6): 539-45

Heape W. The “sexual season” of mammals and the relation of the “pro-oestrum” to menstruation. Q J Microsc Sci. 1900;44:1–70.

Heykants M, Mahabir E. Estrous cycle staging before mating led to increased efficiency in the production of pseudopregnant recipients without negatively affecting embryo transfer in mice. Theriogenology. 2016; 5: 813-21.

Huijbers IJ, Del Bravo J, Bin Ali R, Pritchard C, Braumuller TM, van Miltenburg MH, Henneman L, Michalak EM, Berns A, Jonkers J. Using the GEMM-ESC strategy to study gene function in mouse models. Nat Protoc. 2015 Nov;10(11):1755-85.

Holt WV, Pickard AR. Role of reproductive technologies and genetic resource banks in animal conservation. Rev Reprod. 1999; 4: 143–150.

IBM developerWorks (2015) Bonferroni with Mann-Whitney?. Accessed https://www.ibm.com/developerworks/community/forums/html/topic?id=51942182- 1ad0-4f26-9a49-56849775ac4f. Accessed in May 10th, 2022

Inyawilert W, Liao YJ, Tang PC. Superovulation at a specific stage of the estrous cycle determines the reproductive performance in mice. Reprod Biol. 2016 Dec;16(4):279-286.

Jaramillo LM, Balcazar IB, Duran C. Using vaginal wall impedance to determine estrous cycle phase in Lewis rats. Lab Animal. 2012; 41:122–8.

Jinek M, Chylinski K, Fonfara I, Hauer M, Doudna JA, Charpentier E. A programmable dual-RNA-guided DNA endonuclease in adaptive bacterial immunity. Science. 2012; 337: 816-21.

Kirk R. Thomas, Mario R. Capecchi, Site-directed mutagenesis by gene targeting in mouse embryo-derived stem cells. 1987. Cell, Volume 51, Issue 3.

Lane-Petter W. The provision and use of pathogen-free laboratory animals. *Proceedings of the Royal Society of Medicine*. 1962;55(4):253-63

Liu, Y. et al. Artifcial intelligence-based breast cancer nodal metastasis detection: Insights into the black box for pathologists. Arch. Pathol. Lab. Med. 2019; 143, 859–68

Mann MA, Kinsley C, Broida J, Svare B. Infanticide exhibited by female mice: Genetic, developmental and hormonal influences. Physiology & Behavior. 1983; 30 (5), 697-702.

Marcó J, Larralde J. Efecto de la actividad copulatoria en distintos períodos del ciclo ovárico sobre la ovulación y la reproducción en la rata [Effect of copulatory behavior at different periods of the ovarian cycle on ovulation and reproduction in the rat]. Rev Med Univ Navarra. 1981 Dec;25(4):49-52. Spanish.

Meziane H, Ouagazzal A-M, Aubert L, Wietrzych M, Krezel W. 2006. Estrous cycle effects on behavior of C57BL/6J and BALB/cByJ female mice: implications for phenotyping strategies.Genes, Brain and Behaviour. 2007; 6: 192-200.

Miller B, Takahashi J. Central circadian control of female reproductive function. Frontiers in endocrinology. 2014; 4.

Murphy WJ. Being "penny-wise but pound foolish" in cancer immunotherapy research: the urgent need for mouse cancer models to reflect human modifying factors. Journal for ImmunoTherapy of Cancer (2016) 4:88.

Mohan S. 2020. Keras implementation of VGG16 architecture from scratch with dogs vs cat data set. Accessed from https://machinelearningknowledge.ai/keras-implementation-of-vgg16-architecture-from-scratch-with-dogs-vs-cat-data-set/ . Accessed in December 17th, 2021.

Nakamura H, Hosono T, Kumasawa K, Jones CJP, Aplin JD, Kimura T. Vaginal bioelectrical impedance determines uterine receptivity in mice. 2018; 33 (12): 2241-8.

Nelson JF, Felicio LS, Randall PK, Sims C, Finch CE. A longitudinal study of estrous cyclicity in aging C57BL/6J Mice: I. cycle frequency, length and vaginal cytology. Biol Reprod. 1982;27, 327–39.

Nilsback M-E, Zisserman A. 2006. A visual vocabulary for flower classification. Proceedings of the IEEE Conference on Computer Vision and Pattern Recognition (2006). Accessed from https://www.robots.ox.ac.uk/~vgg/data/flowers/17/. December 12 th, 2021.

Oyola MG, Handa RJ. Hypothalamic–pituitary–adrenal and hypothalamic–pituitary–gonadal axes: sex differences in regulation of stress responsivity. Stress, 2017. *20*(5), 476-494.

Pallares P, Gonzalez-Bulnes A. A new method for induction and synchronization of oestrus and fertile ovulations in mice by using exogenous hormones. Lab Anim, 2008. 43(3):295-299.

Parkes AS. The length of the oestrous cycle in the unmated normal mouse: records of one thousand cycles. J Exp Biol. 1928; 5: 371-7.

Rajpurkar P, Irvin J, Zhu K, Yang B, Mehta H, Duan T, Ding D, Bagul A, Langlots C, Sphanskaya K, Lungren MP, Ng AY. CheXNet: Radiologist-Level Pneumonia Detection on Chest X-rays with Deep Learning, 1–7 (2017). https://arXiv .org/1711.05225v3.

Sano K, Matsuda S, Tohyama S, Komura D, Shimizu E, Sutoh C. Deep learning-based classification of the mouse estrous cycle stages. Scientific Reports. 2020; 10: 11714.

Scavizzi, Ferdinando & Bassi, Cristian & Lupini, Laura & Guerriero, Paola & Raspa, Marcello & Sabbioni, Silvia. A comprehensive approach for microbiota and health monitoring in mouse colonies using metagenomic shotgun sequencing. Animal Microbiome. 2021; 3. 10.1186/s42523-021-00113-4.

Schneider MR, Mangels R, Dean MD. The molecular basis and reproductive function(s) of copulatory plugs. Mol Reprod Dev. 2016;83(9):755-767.

Sharpless, Norman E.; DePinho, Ronald A. The mighty mouse: genetically engineered mouse models in cancer drug development. Nature Reviews Drug Discovery. 2006; 5 (9): 741–54.

Simonyan K, and Zisserman A. Very deep convolutional networks for large-scale image recognition. International Conference on Learning Representations, 1–14 (2015). Accessed from https://arXiv.org/1409.1556v6 at December 20th, 2021.

Singletary SJ, Kirsch AJ, Watson J, Karim BO, Huso DL, Hurn PD, Murphy SJ. Lack of correlation of vaginal impedance measurements with hormone levels in the rat. Contemp Top Lab Anim Sci. 2005 Nov;44(6):37-42.

Singh M, Murriel, CL, Johnson L, Genetically Engineered Mouse Models: Closing the Gap between Preclinical Data and Trial Outcomes. Cancer Research. 2012; 72 (11): 2695–2700.

Stockard CR, and Papanicolaou GN. The existence of a typical oestrous cycle in the guinea pig with a study of its histological and physiological changes. Am J Anat. 1917; 22:225–83.

Summa KC, Vitaterna MH, Turek FW Environmental Perturbation of the Circadian Clock Disrupts Pregnancy in the Mouse. PLoS ONE. 2012; 7(5): e37668.

Schally AV, Nagy A, Szepeshazy K. LHRH analogs with cytotoxic radicals. *In* Filicori M, Flamigni C, eds. Treatment with GNRH Analogs: Controversies and Perspectives. 1996. Carnforth, UK, Parthenon, pp 33–44.

Schally AV, Comaru-Schally AM: 1997. Hypothalamic and other peptide hormones. *In* Holland JF, Frei E III, Bast RR Jr, Kufe DE, Morton DL, Weichselbaum RR, eds. Cancer Medicine, 4th ed. Baltimore, Williams and Wilkins, pp 1067–86.

Terkel J. Neuroendocrinology of coitally and noncoitally induced pseudopregnancy. Ann N Y Acad Sci. 1986; 474:76-94.

Urbanski HF, and Ojeda SR. The juvenile-peripubertal transition period in the female rat: Establishment of a diurnal pattern of pulsatile luteinizing hormone secretion. Endocrinology 1985;117:644–49.

Urry L, Wasserman S, Orr R, Cain M, Minorsky P, Jackson RB, Reece JB. Campbell Biology in Focus. 3rd edition. Pearson, Boston Massachusetts

van der Lee S and Boot LM. Spontaneus pseudopregnancy in mice II. Acta Physiol Pharmacol 5; 1956: 213-5.

van der Lee S and Boot LM. Spontaneus pseudopregnancy in mice. Acta Physiol Pharmacol Neerl; 1955: 442-4.

Wei S, Gong Z, An L, Zhang T, Luo Y, Dai H. Closprostenol and eCG influence oestrus synchronization and uterin development in mice. Veterinarni Medicina. 2015; 1: 31-8.

Whitten WK. Modification of the oestrous cycle of the mouse by external stimuli associated with the male. J Endocrinol. 1956; 13: 399-404.

Yoshiki A, Ike F, Mekada K, Kitaura Y, Nakata H, Hiraiwa N, Mochida K, Ijuin M, Kadota M, Murakami A, Ogura A, Abe K, Moriwaki K, Obata Y. The mouse resources at the RIKEN BioResource center. Exp Anim. 2009; 58: 85–96.

Zhang J, Jin N, Ma Y, Lu J, Wang J, Chen S, Wang X. Ovarian stimulation reduces fetal growth by dysregulating uterine natural killer cells in mice. Mol Reprod Dev, 2021; 88, 618– 627.

Chapter 8- Supplementary

Supplementary 1:
VGG16 Model layers:

```
Model: "sequential"
_________________________________________________________________
 Layer (type)                Output Shape              Param #
=================================================================
 conv2d (Conv2D)             (None, 224, 224, 64)      1792

 conv2d_1 (Conv2D)           (None, 224, 224, 64)      36928

 max_pooling2d (MaxPooling2D  (None, 112, 112, 64)     0
 )

 conv2d_2 (Conv2D)           (None, 112, 112, 128)     73856

 conv2d_3 (Conv2D)           (None, 112, 112, 128)     147584

 max_pooling2d_1 (MaxPooling  (None, 56, 56, 128)      0
 2D)

 conv2d_4 (Conv2D)           (None, 56, 56, 256)       295168

 conv2d_5 (Conv2D)           (None, 56, 56, 256)       590080

 conv2d_6 (Conv2D)           (None, 56, 56, 256)       590080

 max_pooling2d_2 (MaxPooling  (None, 28, 28, 256)      0
 2D)

 conv2d_7 (Conv2D)           (None, 28, 28, 512)       1180160

 conv2d_8 (Conv2D)           (None, 28, 28, 512)       2359808

 conv2d_9 (Conv2D)           (None, 28, 28, 512)       2359808

 max_pooling2d_3 (MaxPooling  (None, 14, 14, 512)      0
 2D)

 conv2d_10 (Conv2D)          (None, 14, 14, 512)       2359808

 conv2d_11 (Conv2D)          (None, 14, 14, 512)       2359808

 conv2d_12 (Conv2D)          (None, 14, 14, 512)       2359808

 vgg16 (MaxPooling2D)        (None, 7, 7, 512)         0

 flatten (Flatten)           (None, 25088)             0

 fc1 (Dense)                 (None, 256)               6422784

 fc2 (Dense)                 (None, 128)               32896

 output (Dense)              (None, 1)                 129

=================================================================
Total params: 21,170,497
Trainable params: 21,170,497
Non-trainable params: 0
_________________________________________________________________
```

Supplementary 2:
Machine Learning Test (Developed by Sakumura Lab)

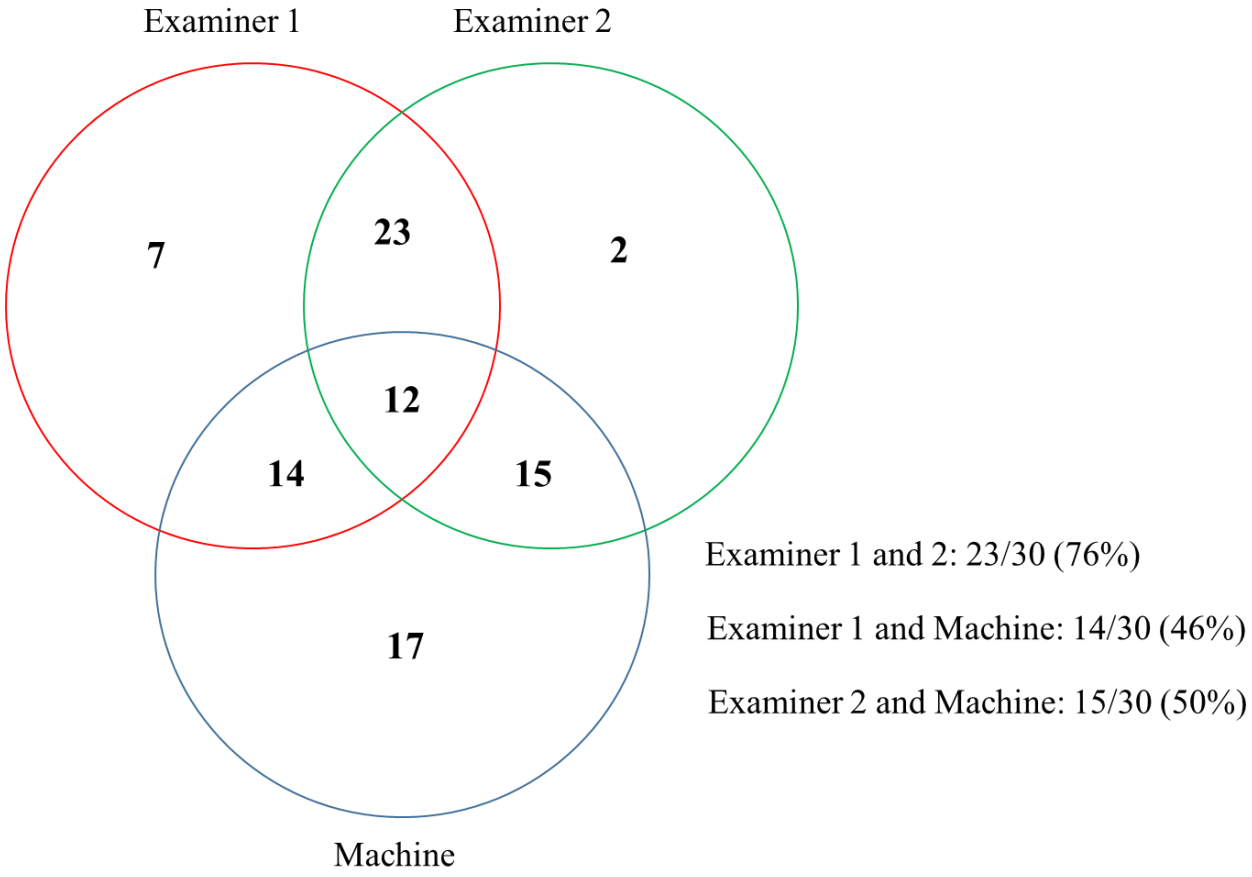

Classification of receptive stages (proestrus-estrus) and non-receptive stages (metestrus-diestrus) of two human examiners and machine.

Supplementary 3:

Embryo transfer using pseudopregnant female mice prepared by LHRHa 2xIP treatment

Method

ES cell culture

R01-09 ESC line was established from embryos by crossing 129X1 female mouse and EGR-R01 ESC (EGR-R01 CAG-mtDsRed2) BDF1x129Sv) derived male mouse. EGR-R01 ESC line was kindly gifted by Dr. Ikawa. The *Ets2* $^{em3/em3}$ ESC line was reported previously (Kishimoto et al., 2021). Establishment of ESC line and maintaining of ESCs were performed as same as previous report (Kishimoto et al., 2021). Both ESC lines were provided for tetraploid complementation.

Tetraploid complementation

Tetraploid embryos were prepared as described previously (Kishimoto et al., 2021; Hirata et al., 2021). In brief, ICR two-cell stage embryos were placed in the fusion buffer, and electrofusion was performed by applying 140 V for 50 ms after aligning embryos between the electrodes. CFB16-HB and LF501PT1-10 electrode (BEXCo.Ltd., Tokyo, Japan) were used for cell fusion. Fused embryos were incubated until use. Six to twelve ESCs were injected into a tetraploid four-cell embryo, and then cultured until the blastocysts stage and transferred into the uterus of E2.5 pseudopregnant ICR mice. Offspring were recovered by natural delivery or Caesarean section on E19.5.

Result

After LHRHa treatment by injection twice by dose 20 μg via intraperitoneal (LHRHa_G3) was confirmed would not affected the embryo development, the ability of pseudopregnant mice that produce with this method as recipient for embryo transfer was examined. After pseudopregnant female mice from LHRHa_G3 were obtained, tetraploid complemented embryos were transferred into their uterus. Offsprings were obtained by natural delivery or Caesarian section on embryonic

day 19.5. Even though few offspring died at birth or until the next day, more than 60% of offspring viability was confirmed (Table Supplementary 3).

Experimental condition	ESC lines	No. of			
		pseudopregnant	transferred	offspring (%)	wean(%)
control[#1]	R01-09	2	40	7 (18)	6 (86)
LHRHa_G3	R01-09	3[#2]	30	7 (23)	5 (71)
	$Ets2^{null(em3/em3)}$		30	9 (30)	6 (67)

[#1] Pseudopregnant female mice of control were prepared by the visual method.
[#2] In all three female mice, ten R01-09 embryos were transferred into the left uteri, and ten Ets2 null (em3/em3) embryos were transferred into the right uteri. R01-09 offspring were recognized by RFP fluorescence signal, and Ets2 null (em3/em3) offspring were recognized by wavy hairs, which is known as Ets2-null mutant phenotype, after 10-day old.

Supplementary 4.
Kruskal-Wallis followed by Bonferroni for litter size, bodyweight, and pregnancy length

A. Litter Size

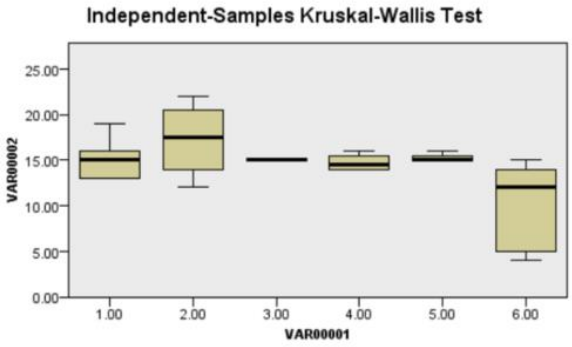

Total N	28
Test Statistic	10.906
Degrees of Freedom	5
Asymptotic Sig. (2-sided test)	.053

1. The test statistic is adjusted for ties.
2. Multiple comparisons are not performed because the overall test does not show significant differences across samples.

B. Bodyweight

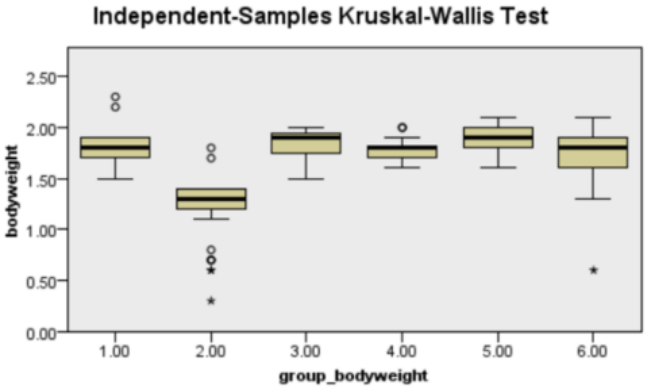

Total N	351
Test Statistic	158.473
Degrees of Freedom	5
Asymptotic Sig. (2-sided test)	.000

1. The test statistic is adjusted for ties.

Each node shows the sample average rank of group_bodyweight.

Sample1-Sample2	Test Statistic	Std. Error	Std. Test Statistic	Sig.	Adj.Sig.
2.00-4.00	-138.752	17.781	-7.803	.000	.000
2.00-6.00	-148.749	16.196	-9.184	.000	.000
2.00-1.00	171.821	15.995	10.742	.000	.000
2.00-3.00	-183.264	28.626	-6.402	.000	.000
2.00-5.00	-208.464	21.955	-9.495	.000	.000
4.00-6.00	-9.997	17.008	-.588	.557	1.000
4.00-1.00	33.069	16.817	1.966	.049	.739
4.00-3.00	44.512	29.093	1.530	.126	1.000
4.00-5.00	-69.712	22.561	-3.090	.002	.030
6.00-1.00	23.072	15.131	1.525	.127	1.000
6.00-3.00	34.515	28.152	1.226	.220	1.000
6.00-5.00	59.715	21.334	2.799	.005	.077
1.00-3.00	-11.443	28.037	-.408	.683	1.000
1.00-5.00	-36.643	21.182	-1.730	.084	1.000
3.00-5.00	-25.200	31.816	-.792	.428	1.000

C. Pregnancy Length

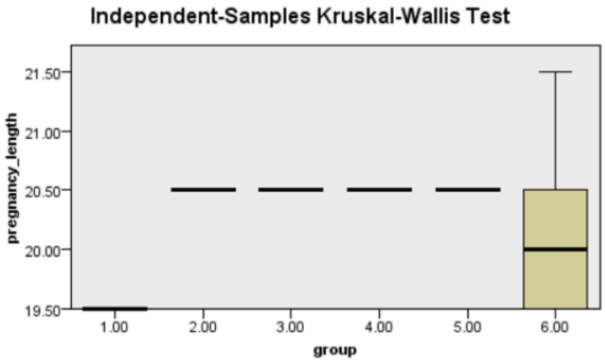

Total N	28
Test Statistic	12.732
Degrees of Freedom	5
Asymptotic Sig. (2-sided test)	.026

1. The test statistic is adjusted for ties.

Each node shows the sample average rank of group.

Sample1-Sample2	Test Statistic	Std. Error	Std. Test Statistic	Sig.	Adj.Sig.
1.00-6.00	-8.200	3.767	-2.177	.029	.442
1.00-2.00	-13.000	4.708	-2.761	.006	.086
1.00-3.00	-13.000	7.879	-1.650	.099	1.000
1.00-4.00	-13.000	4.708	-2.761	.006	.086
1.00-5.00	-13.000	5.158	-2.521	.012	.176
6.00-2.00	4.800	4.315	1.112	.266	1.000
6.00-3.00	4.800	7.650	.627	.530	1.000
6.00-4.00	4.800	4.315	1.112	.266	1.000
6.00-5.00	4.800	4.802	1.000	.317	1.000
2.00-3.00	.000	8.155	.000	1.000	1.000
2.00-4.00	.000	5.158	.000	1.000	1.000
2.00-5.00	.000	5.571	.000	1.000	1.000
3.00-4.00	.000	8.155	.000	1.000	1.000
3.00-5.00	.000	8.422	.000	1.000	1.000
4.00-5.00	.000	5.571	.000	1.000	1.000

Supplementary Figure 4. Statistical Analysis were performed by Kruskal-Wallis test followed by Bonferroni correction, with $P<0.05$, for (A) litter size, (B) body weight, and (C) survival rate of the offsprings. 1: control; 2: PMSG, 3: Progesteron, 4: LHRHa_G1, 5: LHRHa_G2, 6: LHRHa_G3.

Supplementary 5.
Fisher's Exact Test Result

Fisher Exact Test:

Effect of different dose of LHRHa treatment on ICR mice estrous cycle

Treatment	Control			
	Proestrus	Estrus	Metestrus	Diestrus
0.005 mg	0.2158	0.0055*	0.241	0.792
0.01 mg	0.75	0.0318*	0.7075	0.792
0.02 mg	1	0.0002*	1	0.0072*
0.04 mg	0.75	0.0771	0.4372	1

$P < 0.05$

Fisher Exact Test:

Effect of different hormone treatment on ICR mice estrous cycle

Treatment	Control			
	Proestrus	Estrus	Metestrus	Dietrus
PMSG	1	0.3108	0.4286	0.2621
Progesteron	1	0.6351	1	1
LHRHa_G1	0.5077	0.1092	0.5385	0.0532
LHRHa_G2	0.6254	0.6834	1	0.6891
LHRHa_G3	1	0.2852	1	0.22

$P<0.05$

Fisher Exact Test

Effect of difference hormone treatment embryo development

Treatment	Observation		
	Plug rate	Pregnancy rate	Survival rate
PMSG	0.0351*	0.4545	<0.00001*
Progesteron	0.6244	1	1
LHRHa_G1	1	1	1
LHRHa_G2	1	1	1
LHRHa_G3	0.0731	1	0.0007*

$P<0.05$